Applied Geochemistry 74 (2016) 67–83

Contents lists available at ScienceDirect

Applied Geochemistry

journal homepage: www.elsevier.com/locate/apgeochem

Use of multiple age tracers to estimate groundwater residence times and long-term recharge rates in arid southern Oman

Th. Müller [a, *], K. Osenbrück [b], G. Strauch [a], S. Pavetich [c, 1], K.-S. Al-Mashaikhi [d], C. Herb [e], S. Merchel [c], G. Rugel [c], W. Aeschbach [e], W. Sanford [f]

[a] Department of Hydrogeology, Helmholtz-Centre for Environmental Research – UFZ, Permoserstr. 15, 04318 Leipzig, Germany
[b] Department of Geosciences, University of Tuebingen, Hoelderlinstrasse 12, 72074 Tuebingen, Germany
[c] Helmholtz-Zentrum Dresden-Rossendorf, Helmholtz Institute Freiberg for Resource Technology, 01328 Dresden, Germany
[d] Ministry of Regional Municipalities and Water Resources, Salalah, Sultanate of Oman
[e] Institute of Environmental Physics (IUP), Heidelberg University, 69120 Heidelberg, Germany
[f] US Geological Survey, Mail Stop 431, Reston, VA 20192, USA

ARTICLE INFO

Article history:
Received 6 March 2016
Received in revised form
20 August 2016
Accepted 23 August 2016
Available online 24 August 2016

Keywords:
Groundwater
Stable isotopes
Groundwater residence time
^{14}C
^{4}He
^{36}Cl
Arid region
Groundwater flow
Groundwater recharge

ABSTRACT

Multiple age tracers were measured to estimate groundwater residence times in the regional aquifer system underlying southwestern Oman. This area, known as the Najd, is one of the most arid areas in the world and is planned to be the main agricultural center of the Sultanate of Oman in the near future. The three isotopic age tracers ^{4}He, ^{14}C and ^{36}Cl were measured in waters collected from wells along a line that extended roughly from the Dhofar Mountains near the Arabian Sea northward 400 km into the Empty Quarter of the Arabian Peninsula. The wells sampled were mostly open to the Umm Er Radhuma confined aquifer, although, some were completed in the mostly unconfined Rus aquifer. The combined results from the three tracers indicate the age of the confined groundwater is < 40 ka in the recharge area in the Dhofar Mountains, > 100 ka in the central section north of the mountains, and up to and > one Ma in the Empty Quarter. The ^{14}C data were used to help calibrate the ^{4}He and ^{36}Cl data. Mixing models suggest that long open boreholes north of the mountains compromise ^{14}C-only interpretations there, in contrast to ^{4}He and ^{36}Cl calculations that are less sensitive to borehole mixing. Thus, only the latter two tracers from these more distant wells were considered reliable. In addition to the age tracers, $\delta^{2}H$ and $\delta^{18}O$ data suggest that seasonal monsoon and infrequent tropical cyclones are both substantial contributors to the recharge. The study highlights the advantages of using multiple chemical and isotopic data when estimating groundwater travel times and recharge rates, and differentiating recharge mechanisms.

1. Introduction

Arid and semiarid areas are characterized by limited water resources with groundwater often being the only permanent fresh water available for drinking and irrigation. Current low precipitation and high temperatures greatly limit inputs to these subsurface reservoirs. The climatic conditions of these dry areas have long precluded settlement or farming, the anthropogenic water demand, here as output from the subsurface reservoir, was therefore negligibly low. This has changed within the last century and especially in the last 50 years, mainly because of intensified agricultural production with irrigated groundwater (Siebert et al., 2010; WWAP, 2015). Nowadays, heavy groundwater abstraction is a fact in many arid or semiarid areas worldwide (Foster and Loucks, 2006). Consequently, an imbalance between input (groundwater recharge) and output (groundwater abstraction) occurs, leading to depletion of groundwater levels and reductions of groundwater in storage. Groundwater depletion is widely recognized in many aquifers around the globe (Konikow and Kendy, 2005; Wada et al., 2010; Scanlon et al., 2012; Aeschbach-Hertig and Gleeson, 2012). In arid and semiarid areas the degree of impact is often unclear because datasets on predevelopment conditions, abstraction rates and groundwater levels are often missing; in some cases neither one is available. Similarly, sources and quantities of current

* Corresponding author.
[1] Present address: Department of Nuclear Physics, RSPE, Australian National University, Canberra, Australian Capital Territory 0200, Australia.

http://dx.doi.org/10.1016/j.apgeochem.2016.08.012
0883-2927/

recharge as today's input to the system, the residence times of the bulk of the groundwater in the system, and the size of the groundwater reservoir are usually difficult to assess and in most cases unknown. Furthermore, it has to be taken into account that the reservoirs were most likely filled during more humid periods in the past. These occurred over the last million years, during about 10 glacial periods (Lisiecki and Raymo, 2005).

Arid areas often contain old groundwater because low recharge rates are not sufficient to flush out the aquifers. A number of studies have used environmental isotopes including ^{14}C (Bretzler et al., 2011; Cartwright et al., 2012; Plummer and Glynn, 2013), ^{36}Cl (Guendouz and Michelot, 2006; Mahara et al., 2009), or noble gases (Kulongoski et al., 2008; von Rohden et al., 2010) to estimate current and past recharge rates and the age structure of groundwater systems in arid or semiarid regions. All of these tracers are subject to site-specific problems, such as how to determine the initial concentrations at recharge for ^{14}C (e.g. Kalin, 2000) and ^{36}Cl (Davis et al., 1998) best or how to quantify the subsurface influx of helium (Solomon and Cook, 2000). A well-recognized approach to overcome some of these problems is the combination of the above mentioned (among other) dating tracers (Lehmann et al., 2003; Stadler et al., 2010; Herczeg and Leaney, 2011; Plummer et al., 2012). However, the analysis of these tracers is often costly. Moreover, only a few studies have combined groundwater ages in the range of >5 ka with numerical flow models to provide criteria for an improved water resources management (Sanford et al., 2004).

This lack of knowledge and the associated forecasting uncertainty is one reason for the ongoing and increasing heavy groundwater abstraction in many regions worldwide. This is also the case for the present study site: the Najd region in the southern government Dhofar of the Sultanate of Oman (Fig 1). Previously, ^{14}C data has suggested that the bulk of the groundwater in the region is between 4000 and 40,000 years old and would have been recharged mostly during the last glacial maximum (Clark et al., 1987; Al-Mashaikhi, 2011). However, the ages do not show a systematic pattern or development within the Aquifer system, which makes it difficult to detect recharge areas and to explain the changes in age by the hydraulic gradients in the aquifers. Since it is planned that the Najd region will become the main agricultural area of the Sultanate of Oman in the near future, this lack of knowledge makes it difficult to evaluate and to forecast the impacts of the planned large scale groundwater abstractions on the groundwater system.

^{36}Cl decay and the accumulation of ^{4}He both provide the possibility to calculate groundwater residence times up to the million year range. Both tracers were used in the present study to determine more accurate constraints for the residence times of Najd groundwater. Information on the source of the water, the water type and climatic conditions during recharge were gained from stable isotope and chemistry data.

The main objectives of this study are (1) to assess the suitability of the age tracers ^{4}He, ^{14}C and ^{36}Cl for the age range of the investigated groundwater system, (2) to estimate the groundwater residence time based on a combination of the suitable age tracers, and (3) to assess and elucidate the conditions or processes that may cause discordant ages for the single age tracers.

The mean groundwater residence times and the water sources complement the conceptual model of the Najd flow system, which so far was based on hydraulic information, such as water levels and hydraulic gradients. The refined conceptual model as well as the age data of the present study will be presented elsewhere and will improve the parameterization of a numerical flow model simulating the regional groundwater flow and the recharge history of the Najd aquifer system.

2. Study site and hydrogeological setting

The Najd area, located in the Sultanate of Oman in the southeast of the Arabia Peninsula is an arid area extending north from the Dhofar Mountains out into the Rub Al-Khali desert. The Najd covers an area of approximately 90,000 km^2 and is bounded by its border with Yemen in the west, Saudi Arabia in the north, and the Al-Wusta governorate in the east (Fig. 1).

Dhofar as the administrative region can be divided into three regions: the Najd, the <15 km wide semiarid coastal plain, and the intervening Dhofar Mountains. Whereas the southern part of the Dhofar Mountains has steep slopes, the elevation declines very gently towards the north-east. The terrain in the central Najd is comprised of a stony and sandy plain. Wadi channels, partly representing draining patterns from former pluvial periods, pervade the plain in a south-south-west to north-north-east direction. The northern part of the Najd is covered by large sand dunes, which are part of the Rub Al-Khali desert and extend into the Kingdom of Saudi Arabia (Fig. 1).

The agricultural development in the area started in the 1970's and 1980's when water exploration wells in considerable numbers were drilled. The centers of abstraction are the farm areas in the central Najd, north of the city of Thumrait and the city of Thumrait itself. The abstractions have resulted in falling groundwater levels, with declines reaching 50 m at some locations.

2.1. Climate

The Najd is part of one of the most arid areas in the world, with a mean air temperature of 26.3 °C (station Thumrait 1986–2009) and minimum and maximum values of 6.2 °C and 44.7 °C, respectively (Al-Mashaikhi et al., 2012). In the far northern area of Dhofar (the dunes of the Rub Al-Khali desert) temperatures as high as 50 °C have been reported. On the southern slopes of the Dhofar Mountains, the yearly amount of rainfall has reached 299 mm a^{-1}, many times the rate of the interior area, with a mean value of approximately 30 mm a^{-1} (station Thumrait 1980–2009) (Al-Mashaikhi et al., 2012).

There are indications of more humid conditions in previous times in the south of the Arabian Peninsula, including the Dhofar region in particular (e.g. Clark and Fontes, 1990; Fleitmann and Matter, 2009; Rosenberg et al., 2011). Pluvial wadi channels pervade the ground surface and are observable in the field and on satellite images. These channels begin in the Dhofar Mountains and run in a north-easterly direction. Their course and morphology prove that large, intermittent surface flows have been occurring in the area for a long time.

The annual monsoon with its orographic rainfall distribution is the most reliable source of precipitation for the Dhofar area (Hildebrandt et al., 2007). Today, the monsoon does not reach the Najd but is limited to the south side of the Dhofar Mountains. This is caused by the Dhofar Mountains that block the monsoon airflow towards the interior area and an inversion layer limiting the vertical extent of the cloud cover (Abdul-Wahab, 2003). The monsoon precipitation consists of ongoing light rain, drizzle and mists, which last for a few days up to months (June–September).

The only direct sources of rain to the Najd are rare storm events, so-called cyclones that vary strongly in their spatial and time dimension. They occur infrequently every 3–7 years and can bring heavy rainfall and huge amounts of water to the area in relatively short time periods, lasting hours to days. They sometimes result in heavy surface runoff (Wadi-runoff) lasting for several days, as it was observed for example after cyclone O6-A in October 1992 (Macumber et al., 1995) and in October/November 2011 after tropical cyclone Keila caused heavy rain and floods in Dhofar

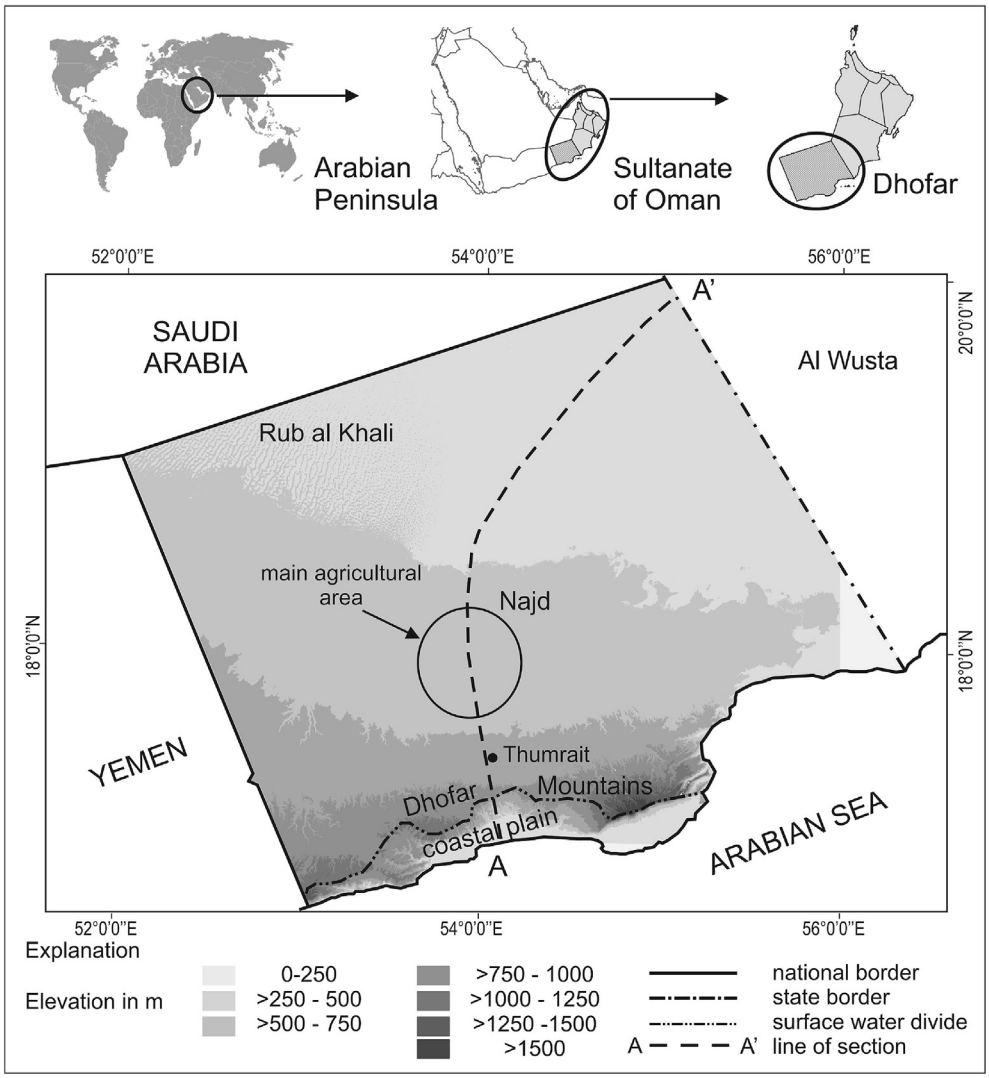

Fig. 1. Map showing study area. The surface water divide in the Dhofar Mountains marks the separation of the semiarid south from the arid Najd. The transect A-A′ is positioned along the generalized groundwater flow direction from the Dhofar Mountains in direction north-east.

(Strauch et al., 2014).

There is evidence that in previous times the position of the Intertropical Convergence Zone (ITCZ) was farther south during the last glacial maximum (LGM) (Weyhenmeyer et al., 2000), and farther north during humid periods (Neff, 2001). This also implies that during humid periods the monsoon precipitation reached farther to the north than today and was able to bring fresh water to the interior area of the Najd.

2.2. Hydrogeologic setting

The formations of interest in the study area are tertiary deposits from the Paleocene and Eocene eras that belong to the Hadramout group, which is present in large areas of the southern and eastern Arabian Peninsula. Predominantly there are up to 900 m thick carbonate sediments, lying unconformably atop Cretaceous formations in the study region. In ascending order, the Hadramout group consists of Paleocene to lower Eocene Umm Er Radhuma ("UER") formations the lower Eocene Rus ("RUS") and the middle to lower Eocene Dammam ("DAM"). The wadi beds of the Hadramout group are partly covered by thin alluvium deposits, which do not act as aquifers. A schematic cross-section (along A-A′ in Fig. 1) of the region with the mentioned geologic formations is shown in Fig. 2.

Underlying the UER is the Shammar Shale of cretaceous origin, comprised of black shale and limestone, which acts as an impermeable layer for the overlying aquifers of the tertiary formations. The thicknesses of the formations are: 50–300 m for the upper UER ("UUER") and 250–300 m for the lower UER ("LUER"), 30–250 m for the RUS and 10–100 m for the DAM. The thickness generally increases in a northeasterly direction. All four formations are mainly comprised of limestone, with varying contents of biomicrite and blue-grey shale (UER), dolomite, marl and gypsum (RUS), and marl and shale (DAM) (Al-Mashaikhi, 2011).

The formations gently dip from the mountains in a northern direction. The UER has outcroppings at the south-side and north-side of the Dhofar Mountains (Fig. 3).

Several geological faults affecting the groundwater dynamics of the region have been mentioned in previous works, for example Clark et al., 1987 or Herb 2011. However, recent seismic surveys by the oil industry did not confirm the occurrence of many of these structures (Al-Mashaikhi, 2011). South to Thumrait evidence of tectonic activity with faults and fold systems have been reported (Mott MacDonald, 1991). According to this study, some of these

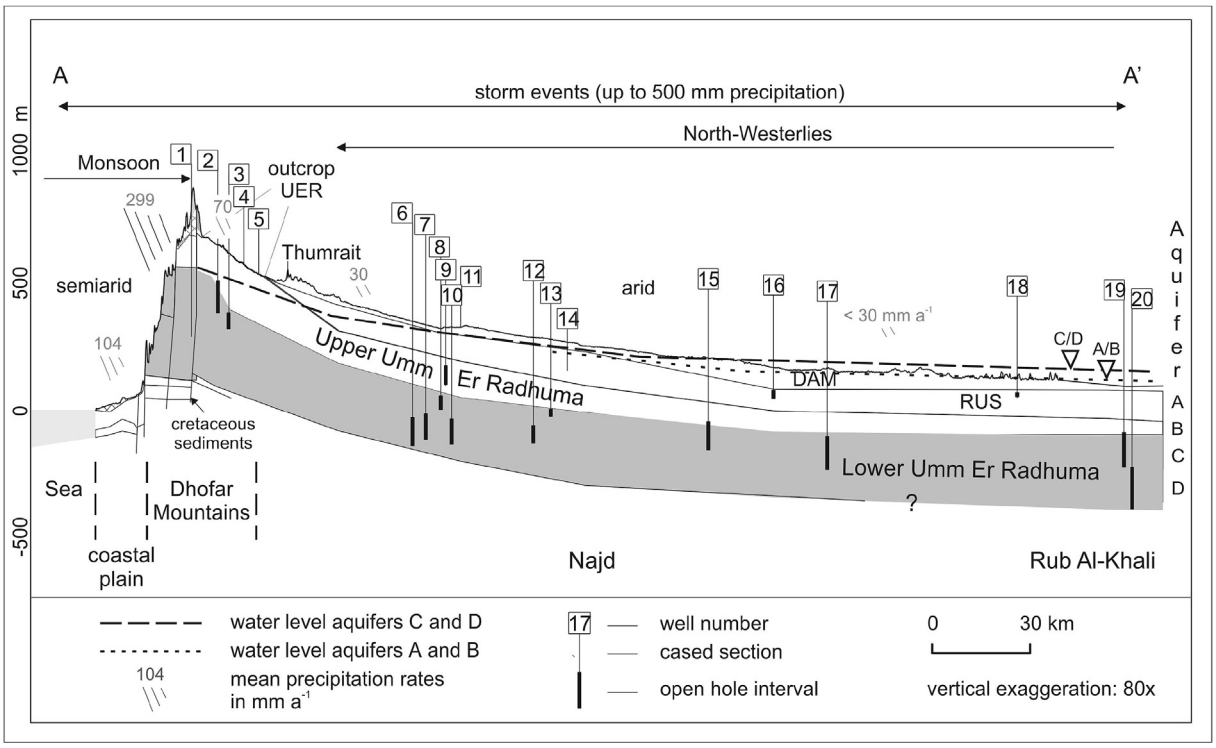

Fig. 2. Cross-section A-A′ along the generalized flow path showing main geologic formations, today's extension of the weather systems and mean precipitation rates. Location and depth of the sampled wells are shown schematically and are not to scale. All four formations are mainly comprised of limestone, with varying contents of biomicrite and blue-grey shale (UER), dolomite, marl and gypsum (RUS) and shale (DAM).

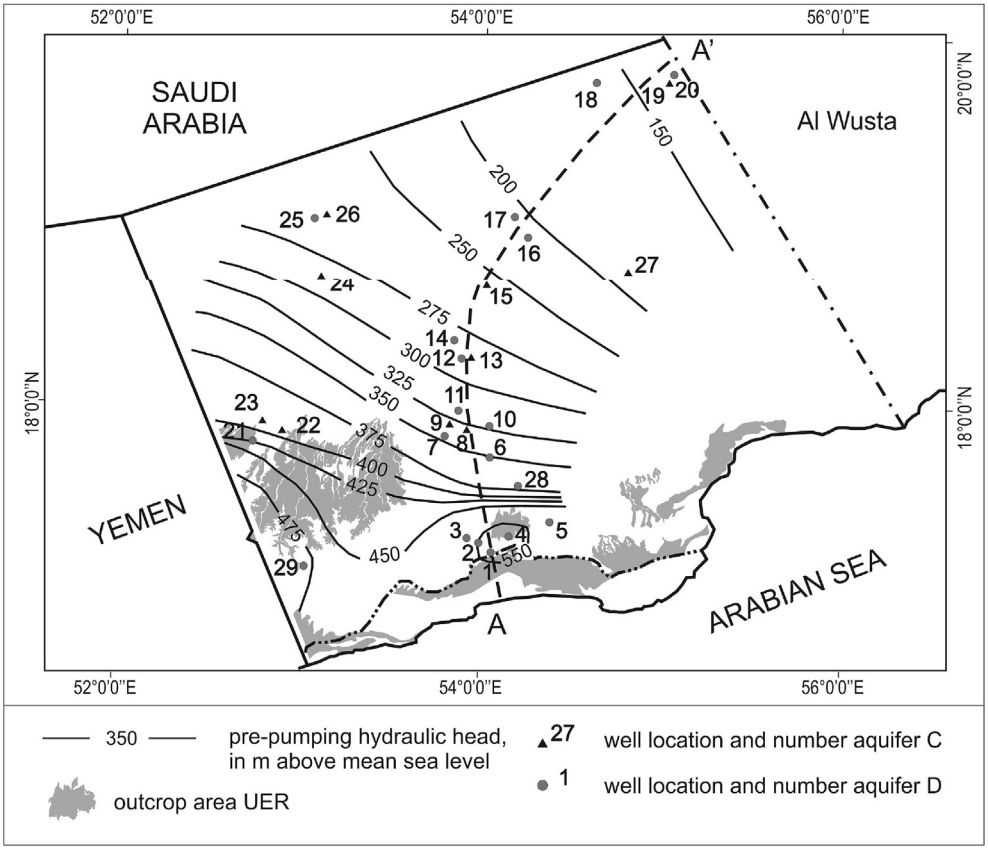

Fig. 3. Predevelopment hydraulic heads in the Najd area for aquifers C and D showing the main groundwater flow direction from the high elevations in the south towards the north-east. The locations of the sampled wells with their numerical identifier are also shown.

faults cut the Precambrian and the Paleozoic-Mesozoic succession, but only a few faults of limited lateral extent cut the lower part of the Tertiary. Moreover, it is argued that fault displacements in the Tertiary are unlikely to form impermeable boundaries within the aquifer (Mott MacDonald, 1991).

Uncertainties also exist about the thickness and separation between formations of the LUER and UUER in the Dhofar Mountains due to cavities of different sizes and depths leading to loss of the drilling cuttings (GRC, 2008).

Four aquifers (A, B, C, D) are known in the Najd (Fig. 2). Aquifer A is unconfined to semi-confined and is located in the DAM and RUS. The aquifers B, C and D are confined and are all located in the UER, with aquifer B in the UUER, and aquifers C and D in the LUER. Aquifers A and B are local aquifers and do not comprise the entire study area. Aquifer A exists mostly in the central Najd area and aquifer B in the central and western Najd. Only aquifer D is distributed over the whole Najd, whereas aquifer C does not extend to the Dhofar Mountains. The city of Thumrait roughly marks the southern border for C. The water bearing horizons are separated by thin layers of shale (Al-Mashaikhi et al., 2012).

Karst features like caverns or doline are visible in the Dhofar Mountains. Loss of drilling, indicating such structures, can be observed in the Mountains but also at some locations in the interior area. Karst features in the Najd are only described for aquifer C (GRC, 2008), while the other aquifers have their water producing zones in fractures and fissures (GRC, 2008; Al-Mashaikhi, 2011).

Transmissivity for all aquifers show a wide range, from tens up to several hundreds m^2/day. Large spatial variations are present in all aquifers. A drilling and aquifer testing program carried out between 2006 and 2008 and targeting on the UER, report mean transmissivities of around 500 m^2/day for aquifers A, B and C, while for aquifer D only 13 m^2/day are given (GRC, 2008). Some works cite even transmissivities >10,000 m^2/day for aquifer C (Clark, 1987; Mott MacDonald, 1991).

It is important to note that in most cases values are derived from short time pumping test (usually less than 1 day). Furthermore a distinction has to be made between early and late transmissivities. (Early transmissivities relate to the first 100 min of the pumping tests, late transmissivities to the time period > 1000 min) It has been shown for the UER in the Najd that early time estimates for transmissivity can be up to two orders of magnitude higher than those resulting from late time data (Mott MacDonald, 1991).

Only limited information on the aquifer porosity for the UER aquifers is available, exhibiting a wide range of values. GRC (2005), for example, present values between 20 and 28% for the LUER, based on geophysical measurements of three wells in the northern Najd. Al-Mashaikhi (2011) cited estimates of 0.5%, and 0.4–10%, respectively, from two earlier studies for the central Najd. Neither of these studies clarified if these values refer to total or effective porosity and how these values were derived. Values of 30% for the total porosity are described for the UER in Saudi Arabia (Bakiewicz et al., 1982), which agrees with a reported typical range of 0–20% for limestone (dolomite) and 5–50% for Karst limestone (Freeze and Cherry, 1979).

2.3. Groundwater flow

The regional (pre-agricultural) groundwater flow in aquifer C and D of the Najd was from the mountains in the south towards north-east. Fig. 3 represents this predevelopment situation constructed from historical water level observations, with highest groundwater levels in the mountains and lower heads downstream. Today's regional flow direction is the same, but cones of depression can be observed at the centers of abstraction.

Higher groundwater levels were observed in aquifers C and D compared to A and B. This characteristic is shown in Fig. 2. Differences in groundwater level up to 50 m are observable in several places. As a result, infiltration of water from the upper aquifers (A and B) to the lower aquifer units (C and D) should be hydraulically impossible in most parts of the study area.

Aquifer C is the main aquifer for groundwater abstraction in the Najd. Flow in aquifer C occurs in the solution channels but also in the matrix. This is indicated by varying drawdowns. Large drawdowns (indicating lower transmissivities or limited extent of the water-bearing horizon) have been observed for example in Thumrait, while in other areas with similar high abstraction rates, the drawdown is smaller.

Increasing groundwater levels in the coastal plain and increasing spring water discharge at the foot of the Dhofar Mountains during and after the monsoon season indicate groundwater recharge south of the surface water divide of the Dhofar Mountains. However, to this date, there are no observations clearly indicating that the monsoon recharge affects or contributes to the groundwater system in the north. In particular, groundwater level observations close to the northern side of the Dhofar Mountains do not exist, and the more distant wells with monitoring records are too far away from the recharge region to be directly influenced by the monsoon events.

3. Methods

The groundwater samples investigated in this study were collected between March 2008 and February 2012. Samples were taken from monitoring wells, public water supply wells and agricultural production wells. In focus of the present study are the wells along the principal cross-section (Fig. 2) from the Dhofar Mountains to northeastern border of Dhofar. Their locations are shown in Fig. 3.

Well depths for the wells in aquifer C and D ranged from 165 to 700 m, with a median of approximately 350 m. The open hole section of the wells ranged from 31 to 270 m with a median of 110 m. The depth to the water table is substantial in the Dhofar Mountains with unsaturated zones more than 200 m thick, but decreases in north-east direction. Approximately halfway between wells 13 and 15 the groundwater in aquifers C and D becomes artesian, meaning they flow at the land surface. In 2008, 2009, 28 wells in all aquifers and one spring in aquifer A were sampled and the water analyzed for ^{14}C and noble gases. In January of 2012, ten wells in aquifer C and D were sampled and analyzed for ^{36}Cl. Detailed information on the sampled wells is given in the Supplementary material (SM Table S1).

Supply and production wells with permanently installed pumps were sampled using taps or valves close to the well head. The artesian wells flowing at the land surface were sampled directly from the well after a sufficient time of open outflow. A submersible pump (MP1) was used to sample wells that were not permanently pumped (*i.e.* monitoring wells). Water was removed from the wells before sampling until constant measured field parameters were observed. Water temperature, electrical conductivity, pH value and the alkalinity were measured during and after sampling (Al-Mashaikhi, 2011; Herb, 2011; Al-Mashaikhi et al., 2012). For the samples discussed here, the field parameters are added in SM Table S2. During field collection, samples were filtered through 0.45 μm cellulose acetate filters, filled in HDPE bottles, acidified using nitric acid to pH 2 for cation analysis, and kept cool at 4 °C. The concentrations of cations and anions were measured at the Department of Analytics and Hydrogeology of the Helmholtz Centre UFZ in Leipzig/Halle, Germany (see SM Ions).

3.1. ^{36}Cl analysis

A total of ten groundwater samples were taken for the analysis of ^{36}Cl in January 2012. The investigation included four samples from aquifer C and six samples from aquifer D (SM Table S1).

Chlorine-36 was measured relative to the stable Cl isotopes, ^{35}Cl and ^{37}Cl, by accelerator mass spectrometry (AMS). The chemical treatment of the samples (Merchel et al. 2013) and the AMS-measurement (Rugel et al., 2016; Pavetich et al., 2014) itself took place at the DREsden AMS (DREAMS) facility (Akhmadaliev et al., 2013) of the Helmholtz-Zentrum Dresden-Rossendorf. Further information is given in the Supplementary Material (SM ^{36}Cl).

3.2. Sampling procedure and analysis for noble gases

Sampling for noble gases took place in November 2009 at 27 wells. Groundwater samples for noble gas analysis were taken in copper tubes (about 40 ml volume) sealed by stainless steel clamps to provide a reliable and durable isolation from the atmosphere. During sampling, any contamination due to contact with the atmosphere was prevented by ensuring a gas-tight connection by flexible tubing between the wells and the sample containers. The entire setup was well-flushed and inspected to remove any gas bubbles.

Noble gas measurements were carried out by mass spectrometry at the Institute of Environmental Physics, University of Heidelberg. The concentrations of the major isotope of each stable noble gas (He, Ne, Ar, Kr, Xe) as well as the isotope ratios $^{3}He/^{4}He$, $^{20}Ne/^{22}Ne$, and $^{40}Ar/^{36}Ar$ were determined. The analytical procedure roughly follows the methods outlined by Beyerle et al. (2000), with specific details described in Friedrich (2007) and Wieser (2010). Concentrations and ratios were subject to inverse modelling (Aeschbach-Hertig et al., 1999; Aeschbach-Hertig et al., 2000). Further information is given in the Supplementary Material (SM Noble gases).

3.3. Carbon isotope analysis

Carbon isotope analyses were carried out by isotope ratio mass spectrometry (IRMS; $\delta^{13}C$) and AMS for ^{14}C at the Institute of Environmental Physics (IUP), University of Heidelberg, Germany. Dissolved inorganic carbon (DIC) was extracted from the water samples using the extraction technique constructed by Unkel (2006) and Kreuzer (2007). Further information is given in the Supplementary Material (SM ^{14}C).

4. Results

4.1. Hydrochemistry of the Najd groundwater

The groundwater chemistry in the different aquifers reflects the geological conditions mentioned. Al-Mashaikhi et al. (2012) presented an overview of the variability of the chemical parameters and mineralization of the groundwater from the four aquifers. Generally, the groundwater mineralization, particularly of aquifer C and D, increases along the flow direction towards the north.

A mean distribution of the predominant major ions of the groundwater from the different Najd aquifers results in a sequence of representative dominant ions in all four Najd aquifers of Cl^- (24.4%) > SO_4^{2-} (21.6%) > HCO_3 (3.0%) and Na^+ (22.6%) > Ca^{2+} (14.9%) > Mg^{2+} (12.2%). These ions comprise more than 98.7% of the dissolved ions in the groundwater, whereas the remaining 1.3% consists of subdominant ions (see SM Table S2). Sodium and chloride concentrations accumulate with increasing distance downward from the surface into deeper aquifers C and D and along the flow path, sulfate concentrations are highest at shallow depths (aquifer A and B), but also in aquifer C in distant wells. The piper plot (see SM – Ions, Fig. S1) shows the dominance of chloride and sodium in aquifer D, additionally sulfate in aquifer C, A and B. Calcium and Magnesium are balanced at higher contents in aquifer C and partly A and D.

Each aquifer can be consequently distinguished by different groundwater types after Al-Mashaikhi et al. (2012): aquifer A is characterized as Na-Ca-SO_4-(Cl), aquifer B as Ca-(Mg)-SO_4, aquifer C as Na-(Mg)-Cl-SO_4, and aquifer D as Na-Cl-SO_4.

4.1.1. Chloride concentration and sources

In this study, the origin and processes affecting chloride concentrations during its transport with the groundwater are of particular importance as ^{36}Cl is used as proxy of groundwater age. Samples from all aquifers show high chloride content (see SM Table S2) as do the samples used for ^{36}Cl analysis.

During the monsoon a chloride concentration of 20 mg L^{-1} was measured in precipitation during the present study. Fog water in the Dhofar Mountains showed a mean value of 44 mg L^{-1} where the values range between 5.6 mg L^{-1} and 84 mg L^{-1} (Schemenauer and Cereceda, 1992). Concentrations in the same range were determined for two cyclonic events in southern Oman (Table 1).

Fig. 4 presents the chloride concentrations along the presumed flowpath in aquifers C and D. Up to kilometre 100 along the flowpath, the chloride concentration in aquifers C and D is higher than in the more distant wells, with a range (apart from well 4) between 100 and 600 mg L^{-1}. The average Cl^- concentration for the samples displayed in Fig. 5 is 327.2 mg L^{-1} for aquifer C (14 samples) and 274 mg L^{-1} for aquifer D (13 samples, the highest value of well 4 was considered as an outlier). Although infiltrating water that contributes to recharge seems to be mainly unaffected by evaporation (as confirmed by stable isotopes of water, see section 4.2), high evaporation rates may lead to the accumulation of chloride in the shallow subsurface after rainfall events with very low precipitation. This chloride may be mobilized during sporadic rainfall events of high intensity (amount and duration) and subsequently be transported to the aquifers under today's climatic conditions. This effect can be confirmed by the following calculation: In the time span 1980 to 1982 twelve rainfall events at station Thumrait (interior Najd) were recorded. Eleven of these events had rainfall amounts between 0.1 and 4.3 mm, one event was recorded with 8 mm. Assuming 20 mg L^{-1} chloride in the rain (according to the referenced values above), complete evaporation would result in the accumulation of 526 mg m^{-2} of chloride in the top soil layer. In February 1983, a heavier rainfall event with 23.3 mm on the 10th and 21.7 mm on the 11th was recorded, which probably washed the accumulated chloride into the ground, leading to potential Cl^- concentrations of several hundred mg L^{-1} in recharging waters.

4.2. Stable isotope pattern of H and O

Today's recharge processes in southern Oman are connected to two water sources of atmospheric origin: (i) the annual monsoon precipitation between June and September; and (ii) periodically appearing tropical cyclones. Monsoon precipitates as rain and fog exclusively at the southern slope and the top area of the Dhofar mountain chain, the region of outcrop of aquifer D. Infrequent tropical cyclones coming from the Arabian Sea and moving across Oman, are the second source. They can cause rainfalls up to more than 400 mm during the transition, resulting in floods along the Wadis up to more than 200 km into the Najd (Strauch et al., 2014). Monsoon and cyclones show distinctive isotopic signatures in their stable water isotopes. Previous studies using this different signature to evaluate the source of the groundwater showed that the

Table 1
Chloride concentration in precipitation and surface water from cyclonic events.

Event	Cl^- in mg L^{-1}			Reference
	Precipitation	Flood water	Pond water	
Cyclone Keila 11/2011	2.1	47.2	86.7 (70 days after the event)	Own measurement; uncertainty <3%
Cyclone O6-A 10/1992			22.0/95.8 (11 days after the event)	Macumber et al. (1995)

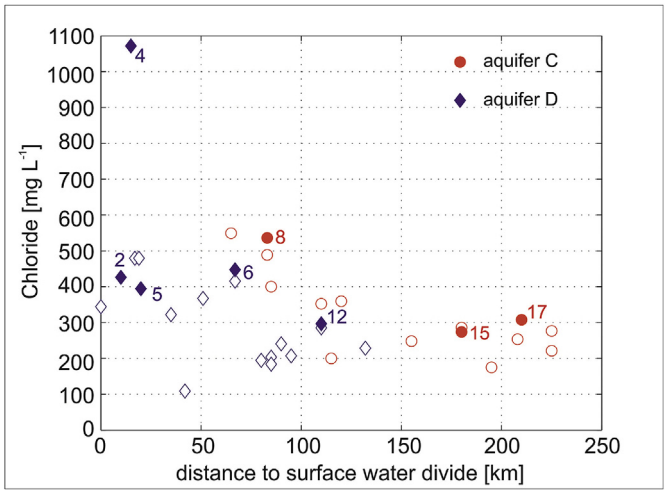

Fig. 4. Chloride concentrations in aquifers C and D in the Najd versus distance from the recharge area. Filled symbols represent wells sampled for ^{36}Cl in 2012, open symbols represent wells sampled 2009. Uncertainty is between 3 and 5%.

respectively. This is clearly distinguishable from monsoon precipitation (Strauch et al., 2014) and confirm the previously observed depleted isotopic composition in ^2H and ^{18}O of cyclones (Macumber et al., 1995).

The groundwater samples of the present study along the selected flow path vary over a wide range between 5‰ and −48‰ in δ^2H and −0.1‰ and −6.2‰ in $\delta^{18}O$ (see Fig. 5 (right) and Table 2). They all plot along the Najd Meteoric Water Line (Al-Mashaikhi et al., 2012). Only samples of aquifer D cover the whole range, while samples of aquifer A and C are significantly depleted (<-30‰ in δ^2H and <-4.5‰ in $\delta^{18}O$). The data of our study confirm the results of Al-Mashaikhi et al. (2012) that are added to Fig. 5 (right).

Samples 1, 2, and 3 are strongly influenced by isotopically-enriched monsoon, while the other samples point into the direction of cyclonic rain water as the main water source. Occurrence of tritium detected in groundwater from the upper aquifer A up to 1.6 TU (Al-Mashaikhi et al., 2012) and up to 9 TU (Clark et al., 1987), confirm that present-day recharge in the shallow Najd aquifers originates from cyclone rain water. The δ^2H and $\delta^{18}O$ values of the four samples of aquifer A (wells 11, 14, 16, 18) fit the range of depleted groundwater < −30‰ in δ^2H and <−4.5‰ in $\delta^{18}O$ as it was

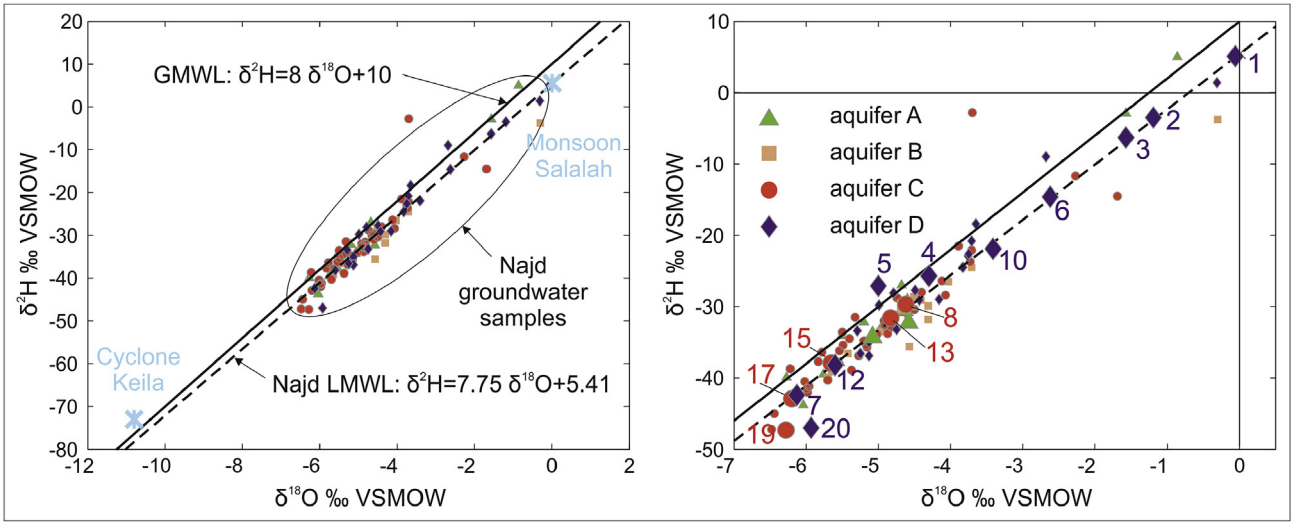

Fig. 5. Left: Stable isotope pattern for precipitation (cyclone and monsoon precipitation after Strauch et al., 2014) and Najd groundwater samples, Local (LMWL) and Global (GMWL) meteoric water line. Right: Relation for the Najd samples used in the present study compared to the majority of the Najd groundwater (small dots, after Al-Mashaikhi et al., 2012).

aquifers in the Najd are comprised mainly of water close to the cyclone signature (Macumber et al., 1995; Al-Mashaikhi et al., 2012; Strauch et al., 2014). The monsoon precipitation varies within a small range between +5 and + 15‰ in δ^2H and −0.4 and 1.5‰ in $\delta^{18}O$, slightly enriched in ^2H compared to the international reference Vienna Standard Mean Ocean Water (VSMOW) being zero ‰ for δ^2H and $\delta^{18}O$ (Strauch et al., 2014). Rain water from the Keila cyclone reaching the southern coast of Oman at October 30, 2011, and sampled on November 4th, 2011, shows strongly depleted water with δ^2H values of −72‰ and $\delta^{18}O$ values −11‰ (Fig. 5, left), reported by Macumber et al. (1995) for a cyclonic rainfall in central Oman in the 1990's. Groundwater of aquifer C, which is not distributed in the recharge area but most likely filled by aquifer D, falls within the range between −30‰ and - 48‰ in δ^2H and −4.6‰ to −6.2‰ in $\delta^{18}O$, respectively, and by that also in the range of cyclone water.

Plotting δ^2H and $\delta^{18}O$ values versus distance along the flow path, there is a clear trend of isotopic depleted groundwater with increasing flow distance (Fig. 6). Groundwater is enriched in ^2H-^{18}O in aquifer D near the Dhofar mountain chain showing a monsoon

Table 2
Results of the isotope analysis.

Site-ID	Sampl. year	Aquifer	$\delta^{18}O$ [‰]	$\delta^{2}H$ [‰]	d-excess [‰]	Tritium [TU]	$\delta^{13}C$-DIC [‰]	^{14}C-DIC [pmC]	He ($\cdot 10^{-8}$) [cm^{3}STP/g]	Ne/He [−]	$^{3}He/^{4}He$ ($\cdot 10^{-8}$) [cm^{3}STP/g]	$^{4}He_{NA}$[a] ($\cdot 10^{-8}$) [cm^{3}STP/g]	$^{36}Cl/^{35}Cl$ ($\cdot 10^{-15}$)	$^{36}Cl/Cl$ ($\cdot 10^{-15}$)	^{36}Cl ($\cdot 10^{7}$) [atoms]
S1	2008	A				0.6 ± 0.3	−7.7	97.0 ± 1.4							
1	2009	D	−0.1	5	6	<0.5	−6.7	22.8 ± 0.5	12.2 ± 0.1	2.2700 ± 0.0254	80.3 ± 4.0	4.91 ± 0.14			
2	2009	D	−1.2	−3	6	<0.5	−3.7	18.0 ± 0.3	12.9 ± 0.1	1.6800 ± 0.0188	57.6 ± 2.8	7.34 ± 0.14			
2	2012	D											22.6 ± 2.6	17.1 ± 2.0	12.4 ± 1.4
3	2009	D	−1.6	−6	7	<0.5	−1.6	3.2 ± 0.5	17.9 ± 0.2	1.1200 ± 0.0126	32.6 ± 1.6	12.90 ± 0.19			
4	2012	D											37.6 ± 3.7	28.5 ± 2.8	51.9 ± 5.2
5	2009	D	−4.8	−28	10	<0.5	−4.7	51.4 ± 0.3							
5	2012	D											47.9 ± 3.6	36.3 ± 2.8	24.3 ± 1.9
6	2009	D	−2.6	−15	6	<0.5	−1.5	5.7 ± 0.8	566.0 ± 5.7	0.0518 ± 0.0006	1.8 ± 0.1	558.00 ± 5.66			
6	2012	D											15.6 ± 2.3	11.8 ± 1.8	8.9 ± 1.3
7	2009	D	−6.1	−41	7	<0.5	−5.6	14.4 ± 0.3							
8	2009	C	−4.6	−30	7	<0.5	−5.8	7.7 ± 0.3	259.0 ± 2.6	0.0821 ± 0.0009	2.7 ± 0.2	254.00 ± 2.59			
8	2012	C											34.8 ± 3.0	26.4 ± 2.3	24.0 ± 2.1
9	2009	B	−4.6	−30	7	0.8 ± 0.3	−1.3	3.1 ± 0.3	204.0 ± 2.0	0.1060 ± 0.0012	2.7 ± 0.2	198.00 ± 1.98			
10	2009	D	−3.4	−22	5	<0.5	−4.8	52.8 ± 0.3							
11	2009	A	−5.1	−34	6	<0.5	−8.4	28.1 ± 0.8	7.6 ± 0.1	2.5900 ± 0.0290	92.8 ± 3.4	2.45 ± 0.09			
12	2009	D	−5.6	−38	7	<0.5	−8.2	44.7 ± 0.3	237.0 ± 3.7	0.0814 ± 0.0013	2.9 ± 0.2	232.00 ± 3.74			
12	2012	D											18.6 ± 2.4	14.1 ± 1.8	7.1 ± 0.9
13	2009	C	−4.8	−32	7	<0.5	−1.4	5.2 ± 0.5	400.0 ± 4.0	0.0599 ± 0.0007	2.5 ± 0.2	393.00 ± 4.00			
14	2009	A	−4.6	−30	7	<0.5	−7.3	45.6 ± 1.6	6.2 ± 0.1	2.9800 ± 0.0334	109.0 ± 1.5	1.47 ± 0.07			
15	2012	C											20.1 ± 2.2	15.2 ± 1.6	7.1 ± 0.8
16	2009	A	−4.7	−30	7	<0.5	−9.4	15.8 ± 0.3	4.7 ± 0.0	3.7100 ± 0.0415	127.0 ± 6.2	0.24 ± 0.05			
17	2009	C	−6.2	−43	6	<0.5	−2.7	10.4 ± 0.3	1450.0 ± 31.8	0.0170 ± 0.0004	1.4 ± 0.2	1440.00 ± 31.80			
17	2012	C											12.8 ± 1.8	9.7 ± 1.4	5.1 ± 0.7
18	2009	A	−4.6	−32	4	<0.5	−9.8	9.9 ± 0.3	5.0 ± 0.1	3.6000 ± 0.0403	120.0 ± 5.9	0.37 ± 0.06			
19	2009	C	−6.2	−48	2	<0.5	−2.0	5.4 ± 0.3	2900.0 ± 29.0	0.0065 ± 0.0001	0.9 ± 0.1	2890.00 ± 29.00			
19	2012	C											12.6 ± 1.7	9.5 ± 1.3	40.2 ± 5.3
20	2009	D	−5.9	−47	0	<0.5	−1.3	5.0 ± 0.3	2580.0 ± 25.8	0.0069 ± 0.0001	1.3 ± 0.1	2580.00 ± 25.80			
20	2012	D											15.8 ± 2.0	11.9 ± 1.5	106.4 ± 13.3
22	2009	C	−3.7	−24	6	<0.5	−4.0	1.7 ± 0.3	1.1 ± 20.4	0.1820 ± 0.0020	6.1 ± 0.3	107.00 ± 1.12			
23	2009	C	−3.7	−22	8	<0.5	−4.2	1.6 ± 0.3	30.3 ± 0.3	0.6810 ± 0.0076	22.6 ± 0.9	25.10 ± 0.31			
24	2009	C	−4.9	−34	5	<0.5	−3.0	9.0 ± 0.3	795.0 ± 8.0	0.0254 ± 0.0003	2.0 ± 0.2	789.00 ± 7.95			
25	2009	D	−5.1	−36	5	<0.5	−2.8	5.1 ± 0.3	1450.0 ± 14.5	0.0145 ± 0.0002	1.5 ± 0.1	1450.00 ± 14.50			
26	2009	C	−5.3	−37	6	<0.5	−2.8	19.4 ± 0.3							
27	2009	C	−5.8	−41	6	<0.5	−9.5	77.2 ± 0.3							
28	2009	D	−3.8	−21	9	<0.5	−4.3	35.8 ± 0.3							
29	2008	D	−4.5	−28	8	1.3 ± 0.4	−8.3	34.6 ± 0.3							

[a] Non-atmospheric ^{4}He.

influence. Large variations in $\delta^{2}H$ and $\delta^{18}O$ (as analyzed recently during cyclone Keila) are observed along the first 80 km northward, while groundwater strongly depleted in $\delta^{2}H$ and $\delta^{18}O$ is observed in the far north-east.

4.3. ^{14}C – data of Najd groundwater

The measured ^{14}C-concentrations in DIC in the groundwater of aquifers C and D range from 1.6 to 77.7 pmC (Table 2). Aquifer D

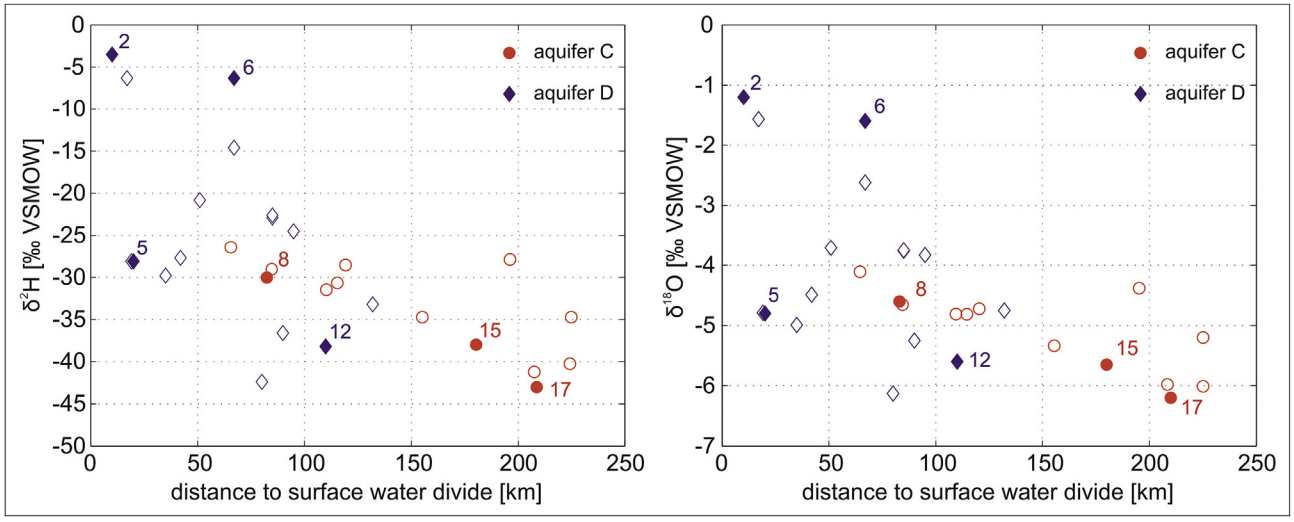

Fig. 6. $\delta^{2}H$ and $\delta^{18}O$ versus distance along the assumed groundwater flow direction. Filled symbols represent wells sampled 2012, open symbols represent all wells from the sampling campaign 2009.

outcrops near the assumed recharge area of the deep Najd groundwater in the Dhofar Mountains. In this area, high ^{14}C-DIC values of 18–51.4 pmC can be attributed to modern groundwater recharge. Lower ^{14}C-DIC values were found in most wells in aquifers C and D downstream the recharge area, but a general trend of decreasing ^{14}C-DIC concentrations in the flow direction cannot be observed. While some wells in the central part of the Najd show the expected lower ^{14}C-DIC concentrations, some wells show similarly high ^{14}C-DIC values as observed in the Dhofar Mountains. The $\delta^{13}C_{DIC}$ values of groundwater from aquifers C and D range from −1‰ to −8‰ which is in accordance with an expected mixture of DIC from soil CO_2 (average $\delta^{13}C_{CO2}$ of −18‰ ± 3‰ based on four measurements in the recharge area) and from carbonates of the aquifer matrix (average $\delta^{13}C_{Carb}$ of +2.7‰ ± 0.6‰ based on five drilling cores). Though $\delta^{13}C_{DIC}$ values generally increase with decreasing 14C-DIC, no significant trend is observable, particularly not for the anomalous ^{14}C-DIC values.

In view of the irregular distribution of transmissivity in the aquifers, we cannot expect to observe a simple pattern of increasing age with distance from the mountains. Some irregularities in the age distribution were already observed by Clark et al. (1987). However, in contrast to that study, we observe very high ^{14}C-DIC activities in some more distal wells of aquifers C and D that can hardly be reconciled with the concept of the deep Najd groundwater flowing in northeasterly direction. While the most ^{14}C correction models account for lowering of ^{14}C-DIC activities by dilution with ^{14}C-free carbon (e.g., from dissolution of carbonates), there is no simple way to explain high ^{14}C concentrations in supposedly old groundwater. The high ^{14}C-DIC activities in the distal wells of aquifers C and D (especially wells 26, 27 (C) and 12, 13 (D)) cannot be explained by contributions from modern recharge. Local infiltration of modern water seems to be unlikely, taking into account the arid conditions and, hence, limited rainfall amounts in the Najd as well as the upward gradient from aquifer D to the upper aquifers and the artesian conditions, which exist from the central Najd in northern direction. Influence of pumping can almost be excluded for wells 26 and 27, as both wells are far away from farming areas. Wells 12 and 13 (aquifer D) on the other hand, are close to today's abstraction areas. Although, aquifer D is not the targeted aquifer for the farming activities, we do not know if, or to what extent, pumping from aquifer C might influence aquifer D. At this point, no satisfying explanation for the high ^{14}C-DIC concentrations along the groundwater flow path can be given. Moreover, we cannot rule out that the processes that influenced the wells in the far north, also affect groundwater of aquifer C and D in the central part of the Najd. Possible reasons for the high ^{14}C-DIC concentrations in aquifers C and D are: (1) local reversal of pressure gradients inducing inflow of younger groundwater due to recent increase in water extraction, (2) admixture of young groundwater from aquifers A and/or B within the borehole due to long open intervals and lacking seals between the aquifers (only possible in areas where aquifers A or B are present), (3) diffusion of recent CO_2 from the vadose zone into aquifer C, which may form a significant (young) fraction of the otherwise low HCO_3 concentrations in aquifer C (only possible if aquifers A and B are missing), and (4) contamination with modern carbon, although precautions were taken to avoid air contact during sampling. In addition to an admixture of ^{14}C-containing DIC to the aquifers of interest (C and D), these processes will also affect the concentrations of other age tracers (and their age interpretations) by e.g., dilution of ^{4}He concentrations with ^{4}He-poor groundwater (or loss of ^{4}He into the vadose zone) or increase of ^{36}Cl/Cl ratios from the admixture of ^{36}Cl-containing chlorine.

4.4. ^{4}He data of Najd groundwater

The concentrations of non-atmospheric (n.a.) ^{4}He, calculated by subtracting modeled atmospheric He from the measured He concentrations, vary between 2.42×10^{-9} cm^3 STP g^{-1} (well 16) and 2.89×10^{-5} cm^3 STP g^{-1} (well 19) with the highest concentrations at the far distant wells 19 and 20 (Table 2). Sources of this ^{4}He can be radiogenic helium produced (i) in the aquifer itself ("*in-situ*"), (ii) in the earth's crust ("crustal flux"), or (iii) released by weathering of sediments (Solomon et al., 1996). In addition, (iv) a helium flux from the earth's mantle ($^{4}He_m$) may occur. By using the isotopic composition (^{3}He/^{4}He ratio) the helium sources can be identified; ^{3}He/^{4}He ratios for mantle helium are around 10^{-5} (Ozima and Podosek, 2002), crustal helium is in general in the range of 10^{-9} to 10^{-7}, with a typical value of 2×10^{-8} (Mamyrin and Tolstikhin, 1984), and atmospheric helium has a ^{3}He/^{4}He ratio of 1.384×10^{-6} (Clarke et al., 1976) or 1.36×10^{-6} for air-equilibrated water (Benson and Krause, 1980). Atmospheric helium contribution as contamination dissolved in groundwater can be estimated by ^{20}Ne measurements and corrected using the ^{4}He/^{20}Ne ratio of dissolved air proposed by Craig et al. (1978).

Plotting the ^{3}He/^{4}He ratio over the Ne/He ratio reveals that the Najd samples plot almost all along an ideal two component mixing line between atmospheric and radiogenic end members while influence of $^{4}He_m$ cannot be observed (Fig. 7). Samples of the shallow aquifers A and B show a high atmospheric helium component, whereas the wells in aquifers C and D have a dominating trend to $^{4}He_{rad}$. Apart from the Spring S1, Tritium was detected in one sample of Aquifer A. The tritiogenic ^{3}He concentration of the sample is negative. It is concluded that apart from sample S1all samples of aquifer A are pre-bomb.

Fig. 8 (left) reveals that the increase in $^{4}He_{rad}$ is not a linear function with distance for all Najd wells. Fig. 8 (right) shows the radiogenic concentration over drilled depth. The long open-hole sections of the wells are schematically indicated by the dashed grey lines. Comparing both plots reveals that, apart from well 6 and well 12, the order of the wells is the same. This suggests that distance, and in turn residence times, seems to have a greater influence on the concentration than depth. The distribution in both plots indicates that no major sources of different types, such as local high concentrations of uranium (which would lead to higher

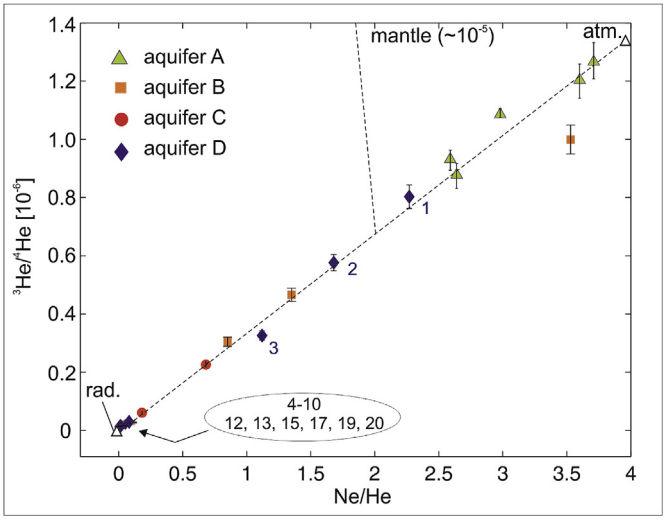

Fig. 7. ^{3}He/^{4}He ratio versus Ne/He ratio to distinguish the different helium end members. Wells along the principal flow line in aquifers C and D are marked with their identifiers.

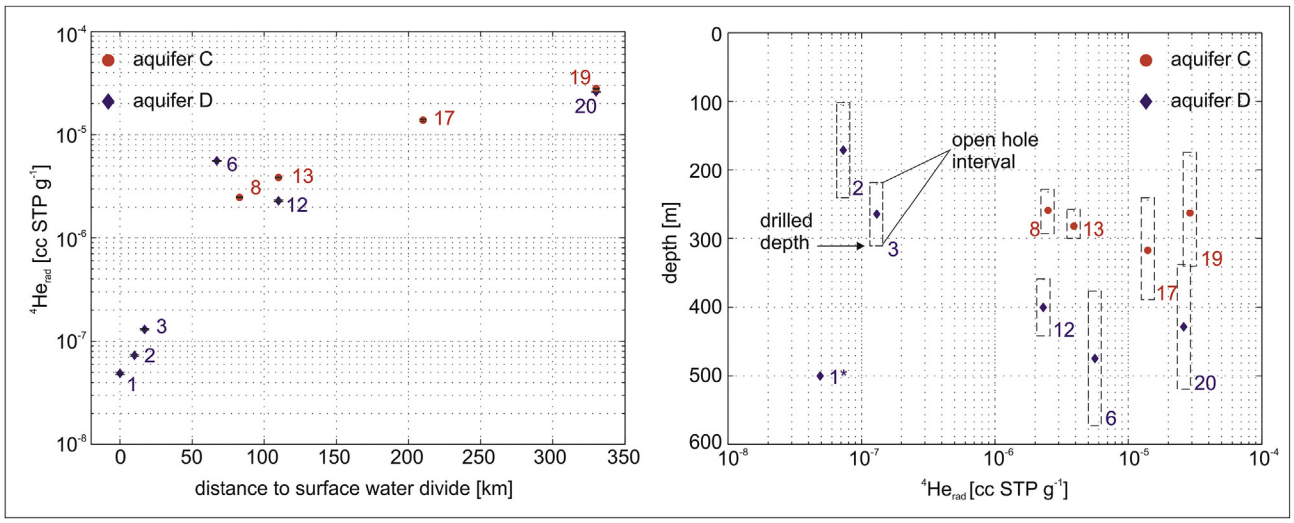

Fig. 8. Distance versus $^4He_{rad}$ (left) and $^4He_{rad}$ against depth (right). $^4He_{rad}$ ranges over three orders of magnitude and is, therefore, plotted on a logarithmic scale. Distance seems to be of greater influence than depth. Left: The increase in $^4He_{rad}$ is not a linear function of distance. Right: Dashed grey lines represent open-hole sections of the wells (1*- no borehole data available).

helium concentrations) influence the helium concentrations in the Najd wells.

The analyzed ^4He data show a trend of increasing non-atmospheric helium concentrations with distance to the assumed recharge area. Unlike the ^{14}C data, this observed trend matches the overall concept of the nature of the Najd groundwater system with a groundwater flow direction from the Dhofar Mountains in direction north east; leading to the conclusion that ^4He might be the more robust tracer for dating of the Najd groundwater. Groundwater with ^4He concentrations above 1.0×10^{-6} ccSTP g^{-1} was sampled in other study areas around the globe before, and could be used for dating groundwater older than 100 ka (e.g. Zuber et al., 1997; Plummer et al., 2012; Sturchio and Purtschert, 2013; Torgersen, 2013). For the Najd groundwater all wells in aquifers C and D outside the recharge area are above this value, pointing in the direction of groundwater residence times beyond the ^{14}C-range.

4.5. ^{36}Cl along the flowpath

Ten wells along the flowpath were sampled for ^{36}Cl analysis in January 2012. Table 2 displays the measured $^{36}Cl/^{35}Cl$ ratio, the calculated $^{36}Cl/Cl$ (expressed as atomic ratio) the number of ^{36}Cl atoms per litre (10^7 at L^{-1}). The blank correction reduces the final $^{36}Cl/^{35}Cl$ values of the samples by 1–5%. The main source of the given uncertainties, which are in the range of 8–15%, are the low counting statistics (7–13%), but also systematic uncertainties like the measured and the theoretical uncertainty of the reference material, the uncertainty from the blank correction and the uncertainty from the sulphur correction are included. All samples show $^{36}Cl/Cl$ ratios below 40×10^{-15}, with the highest values at the beginning of the flowpath and lower values downstream (Fig. 9, left and Table 2). This general decreasing trend of $^{36}Cl/Cl$ ratios with distance agrees with the groundwater flow direction in the Najd. Differences between well 4, 5, and 8 to the other wells are observable. They are higher in both the $^{36}Cl/Cl$ ratios and the ^{36}Cl concentration then expected regarding their position along the flow path. It also has to be mentioned that taking into account the statistical uncertainty, increasing $^{36}Cl/Cl$ ratios cannot be entirely excluded in aquifer D between wells 2 and 12 and 6 and 12. However, apart from well 19 and well 20 the ^{36}Cl concentration decreases along the flow direction as shown in Fig. 9, right, confirming the general decreasing trend of the $^{36}Cl/Cl$ ratio with distance.

The radioactive isotope ^{36}Cl is used for dating very old groundwater, because of its long half-life of $(3.010 \pm 0.015) \times 10^5$ years (Nica et al., 2012). ^{36}Cl of cosmogenic (precipitation) and hypogenic origin (from mineral surfaces) and Cl^- enter the subsurface with infiltrating water. With the water, the atoms move through the soil and the unsaturated zone and, when reaching the saturated zone, are transported by the flowing groundwater. During this time ^{36}Cl decays, leading to lower $^{36}Cl/Cl$ ratios with increasing distance (increasing age) from the recharge area. This decay is used to estimate the time the water has been in the system (Bentley et al. 1986; Phillips et al., 1986; Phillips, 2000). In order to achieve this, the initial concentration has to be estimated (Davis et al., 1998; Scheiber et al., 2015) and it has to be considered that (i) ^{36}Cl can also be added in the deep subsurface by nucleogenic production, (ii) the $^{36}Cl/Cl$ ratio can be influenced by varying Cl^- concentrations (evaporation during recharge or old residing Cl^- in confining layers) (Phillips, 2013) and, (iii), the cosmogenic production and, therefore, the $^{36}Cl/Cl$ ratios changed over time (Plummer et al., 1997; Phillips, 2013). Furthermore the influences of changing climatic conditions have to be noted. They can cause variability in ^{36}Cl in the recharge zone due to changing evapotranspiration (Love et al., 2000). Regarding the timescale up to the Ma range, changing sea levels also affected the distance of the marine (Cl^-) source from the recharge zone (Bentley et al., 1986; Purdy et al., 1996; Scheiber et al., 2015).

Our interpretation is that the $^{36}Cl/Cl$ decrease from the wells in the Dhofar Mountains to the wells downstream is due to radioactive decay along the direction of the groundwater flow. The high ^{36}Cl at wells 19 and 20 could be an indication for enhanced subsurface production, strong evaporation effects or leakage from old water from the confining layers. Alternatively, different groundwater flow velocities subparallel to the general flow direction would create some variability in the overall decreasing $^{36}Cl/Cl$ trend with distance.

5. Groundwater residence times

5.1. Groundwater residence times based on ^{14}C

Groundwater in the limestone aquifers of the Najd is obviously prone to reservoir effects due to the dissolution of old carbonates.

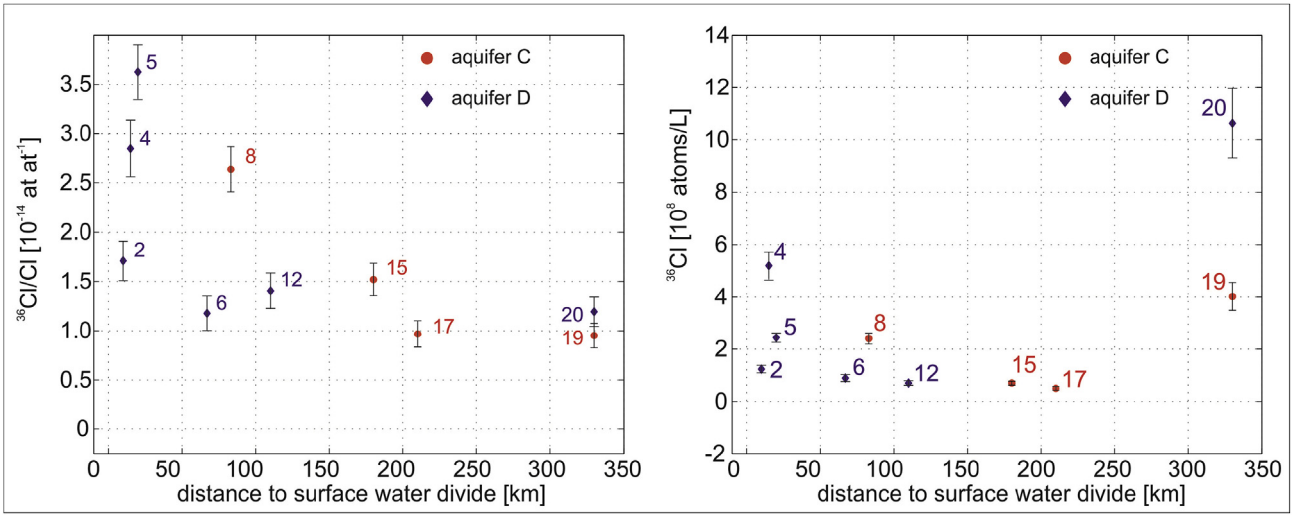

Fig. 9. Left: ^{36}Cl/Cl with total uncertainties (dominated by statistical uncertainty) plotted against distance. Right: ^{36}Cl concentrations versus distance. 0 km represents the surface water divide in the Dhofar Mountains.

Measured values of $\delta^{13}C_{Carb}$ scatter around the typical oceanic value of 0‰, addition from carbon from this source should thus lead to enriched $\delta^{13}C$ values of the DIC. Indeed, the $\delta^{13}C$ values (Table 2) are quite high and can reach up to near zero values. As a result, the usual $\delta^{13}C$-based correction models predict strongly reduced initial ^{14}C activities, making even the samples with the lowest ^{14}C activities of few pmC appear rather young. These strong corrections, however, come with large uncertainty, as different models and assumptions on e.g. soil gas and carbonate $\delta^{13}C$-values yield quite different results. Even more problematic is the finding of high ^{14}C activities in some distant wells, indicating an apparent admixing of young carbon from an unknown source, which potentially could bias all ^{14}C data and hence makes any attempts for detailed 14C-dating using complex models quite futile. The wells least affected by an apparent admixture of ^{14}C-DIC are probably locations near the recharge area (wells 1, 2, and 3). For this reason, ^{14}C-DIC-based groundwater ages were only estimated for these three wells. The ^{14}C ages were calculated by inverse modelling of the geochemical mass balance along presumed groundwater flowpaths using the model code NETPATH (Plummer et al., 1994). For modelling, we consider the chemical and isotopic composition of recently recharged groundwater as initial composition and its geochemical evolution towards the wells 1, 2, and 3 as final composition. In order to account for uncertainties in the initial composition, two different waters were taken into account: (1) the spring S1 located close to the watershed and (2) a hypothetical recharge water defined by saturation indices of −1 for calcite, −2 for dolomite, and −3 for gypsum, at a partial CO_2 pressure of $10^{-2.5}$. The major changes in water chemistry along the presumed flowpath can be attributed to the dissolution of gypsum and dolomite, the precipitation of calcite, and ion exchange processes. The derived ^{14}C ages are (7.3 ± 2.0) ka for well 1, (4.4 ± 2.0) ka for well 2 and (17.2 ± 1.0) ka for well 3. The errors represent the age range obtained from all models in accordance with the chemical and isotopic data for both initial compositions.

5.2. Groundwater residence times based on non-atmospheric ^4He

The isotope plot (Fig. 7) showed that no mantle Helium (^4He_m) is present in the Najd groundwater samples. For the radiogenic ^4He no distinction can be made between the helium that is produced within the aquifer (*in-situ*) or results from an external flux into the aquifer from the earth's crust ("crustal flux"). Both are produced by the α-decay of U and Th contained in the rock matrix (Andrews and Lee, 1979; Stute et al., 1992). The simplest approach for the calculation of the groundwater residence times is a single ^4He source (*in-situ* produced ^4He) with a constant production rate throughout the aquifer. By further using the aquifer's porosity and assuming complete release of He from the sediment, a He accumulation rate in the groundwater can be calculated (e.g. Castro et al., 2000; Kipfer et al., 2002).

Values for U and Th for five samples for the LUER have been analyzed and averaged to (1.26 ± 0.34) μg g^{-1} and (0.11 ± 0.11) μg g^{-1}. Measurements for total or effective porosity were not available for UER aquifer. Assuming a value of 10% the He accumulation rate is (3.6 ± 1.0) × 10^{-12} cm^3 STP g^{-1} a^{-1}. This value is within the range from the literature, for example (3.95 × 10^{-12} to 6.2 × 10^{-12}) cm^3 STP g^{-1} a^{-1} for the Great Artesian Basin in Australia (Torgersen and Clarke, 1985), (1.6 ± 0.2) × 10^{-12} cm^3 STP g^{-1} a^{-1} for the Aquia Aquifer in Maryland in the USA (Aeschbach-Hertig et al., 2002), or (2.8 ± 1.8) × 10^{-12} cm^3 STP g^{-1} a^{-1} for the upper Patapsco aquifer in Maryland (Plummer et al., 2012).

A main problem with this approach is the large uncertainty about the applicable values for the (effective) porosity for the aquifers in the Najd. With the before-mentioned values between 1% and 30% the estimated accumulation rate varies by more than one order of magnitude (4.0 × 10^{-11} to 9.4 × 10^{-13} cm^3 STP g^{-1} a^{-1}).

Due to this uncertainty we estimated the ^4He *in-situ* accumulation rate by using ^{14}C-ages and the analyzed ^4He concentrations of wells 1, 2, and 3 in the recharge area. This approach was used before (Plummer et al., 2012) for the upper Patapsco aquifer in Maryland. Using the ^{14}C ages of the wells 1 ((7.3 ± 2.0) ka), 2 ((4.4 ± 2.0) ka) and 3 ((17.2 ± 1.0) ka), an average ^4He accumulation rate of (1.1 ± 0.8) × 10^{-11} cm^3 STP g^{-1} a^{-1} was calculated. This value is compatible with the above presented numbers based on measured U and Th concentrations, but would point to quite low porosity values. In fact, ^4He accumulation rates in the order of 10^{-11} cm^3 STP g^{-1} a^{-1} could only be calculated for porosities below 5%. Applying the ^{14}C-derived ^4He production rate ((1.1 ± 0.8) × 10^{-11}cm^3 STP g^{-1} a^{-1}) to the entire aquifer system, results in ^4He ages in aquifers C and D up to 350 ka in the central Najd, and in the Ma range for the far distant wells along the principal flow path (Table 3). These initially calculated (*in-situ*) ^4He ages for the Najd differ significantly from the age range given by the ^{14}C

Table 3
Calculated ^{4}He-model ages (ka) considering only *in-situ* production within the aquifer.

Recharge area				Central Dhofar				North-east Dhofar			
Well	^{4}He-age [ka]			Well	^{4}He-age [ka]			Well	^{4}He-age [ka]		
	Min	Mean	Max		Min	Mean	Max		Min	Mean	Max
1	2	4	15	6[a]	282	487	1.700	17	720	1.260	4.436
2	4	6	22	8	128	222	773	19	1.461	2.524	8.800
3	6	11	40	12	117	203	711	20	1.304	2.253	7.855
				13	199	343	1.200				

[a] Well 6 is not used for interpretation because the well is drilled up to the bottom of the LUER and was heavily pumped for industrial use for several years.

data in previous studies (Clark, 1987). This also applies when considering the uncertainties for ^{4}He and the ^{14}C ages as the minimum and maximum ages. Furthermore it has to be taken into account that the ^{14}C-derived ^{4}He production rate is half an order of magnitude above the mentioned literature values. A lower ^{4}He *in-situ* accumulation rate would result in even higher ^{4}He ages.

The high ^{4}He ages estimated (based on *in-situ* production only) could indicate that an additional helium source may be present. Assuming that the $^4He_{rad}$ in the aquifers is the result of *in-situ* produced ^{4}He plus a ^{4}He flux from outside the aquifer, would result in lower groundwater residence times. Torgersen and Clarke (1985) showed how the helium evolution in the aquifer as a function of distance and depth within the aquifer can be calculated when two $^4He_{rad}$ sources exist. Comparing the $^4He_{rad}$ concentrations calculated by such a model with measured values in principle also enables an estimation of groundwater flow velocities and ages. However, again a large uncertainty arises from the wide range of possible input parameters for the model. Torgersen (2010) gives a variability of crustal flux that is as high as ± 1.5 orders of magnitude. The same order probably applies to the other parameters (porosity, diffusion coefficient) as well. Overall, the number of degrees of freedom in modelling the concentrations of $^4He_{rad}$ in the aquifer system resulting from both *in-situ* production and an external flux is too big to calculate He-based groundwater residence times with reasonable precision.

However, an observable trend is the accumulation of ^{4}He along the flowpath. Therefore, ^{4}He may be used for qualitative dating of the Najd groundwater, *i.e.* higher ^{4}He indicating higher groundwater residence times, whereas for the quantitative dating too many uncertainties exist.

5.3. Dating of Najd groundwater by ^{36}Cl decay

Interpreting the ^{36}Cl evolution of the Najd groundwater by decay, the residence time of the groundwater can be calculated by (Phillips et al., 1986, 2013; Bentley et al., 1986):

$$t = \frac{-1}{\lambda 36} \ln \frac{R - R_{se}}{R_0 - R_{se}} \quad (1)$$

when assuming meteoric input as the only source for ^{36}Cl and decay as the only sink. Here, R is the measured ^{36}Cl/Cl ratio, R_o the initial ^{36}Cl/Cl ratio, and R_{se} the secular equilibrium ^{36}Cl/Cl ratio.

It is also possible that at the same time ^{36}Cl or Cl^- could be accumulated underground from *in-situ* sources. For this case, the right term of Equation (1) is extended by the ratio of C, as the sampled concentration of chloride, and C_o as the concentration of chloride in recharge:

$$t = \frac{-1}{\lambda 36} \ln \frac{C(R - R_{se})}{C_0(R_0 - R_{se})} \quad (2)$$

Using Equation (2) for dating the Najd groundwater requires, in addition to the analyzed values, the initial ^{36}Cl/Cl ratio and the secular equilibrium ratio (R_{se}). For the initial ^{36}Cl/Cl ratio no measurements of ^{36}Cl for rain, shallow groundwater samples or soil profiles from the recharge area were available. We decided to take the value of well 2 as the initial ratio. The location at the beginning of the flowpath and the low ^{4}He concentration permit the conclusion. Compared to well 2, well 8 has a quite high ^{4}He concentration – pointing to a much longer residence time in the system. On the other hand, well 8 (and wells 4 and 5) show a higher ^{36}Cl/Cl ratio. Interpreting this higher ^{36}Cl/Cl ratio as younger water would be contrary to the ^{4}He interpretation. We believe that the water of wells 4, 5 and 8 were recharged under different conditions, such as a different recharge system during times of low sea-level stand and a resulting greater distance of the Najd to the sea, or higher ^{36}Cl/Cl ratios in rainfall due to a stronger continental influence. For this reason wells 4, 5 and 8 will not be considered in the ^{36}Cl calculations. The secular equilibrium ratio R_{Se} at equilibrium with the subsurface neutron flux (φ), requires knowledge of the subsurface flux which in turn requires values for uranium and thorium as well as specific coefficients of the rock material (Schimmelpfennig et al., 2009). With the above given values for U and Th and literature values for the other required parameters, the secular equilibrium would result in a value between 3.47 and 12.8 × 10^{-15} ^{36}Cl/Cl. The secular equilibrium should not be above the smallest measured ^{36}Cl/Cl ratio. This is the case for the Najd samples with (9.5 ± 1.3) × 10^{-15} at at^{-1} as the smallest value at well 19. Both, the calculated range and the sample of well 19, fit the literature values, for example Phillips (2000) suggested (8 ± 3) × 10^{-15} at at^{-1}.

Given these estimates, Equation (2) was used to calculate the residence times by ^{36}Cl decay for the wells 12, 15 and 17 in the central area of the Najd. Well 6 was again excluded for the above given reasons, samples of well 19 and 20 were not considered because of their unknown ^{36}Cl origin. The ^{36}Cl ages were calculated with an initial value of 17.1 × 10^{-15} at at^{-1} and a recharge Cl^- concentration of 302 mg L^{-1} as the average of all samples of aquifers C and D (see Table S2 in SM). Using R_{se} = 0 for the calculation results in minimum ages, and R_{se}=(9.5 ± 1.3) × 10^{-15} at at^{-1} (as the lowest ^{36}Cl/Cl ratio analyzed) was used for the calculation of the maximum ages.

The age estimates again range above the ^{14}C -range but back-up the ^{4}He-ages. When considering the analytical uncertainty, a minimum ^{36}Cl –age of 41 ka and a maximum ^{36}Cl -age of more than 1.6 Ma were calculated. For the central area (well 12, approximately 110 km inland) the ^{36}Cl-based residence times range between 41 and 450 ka. Almost the same range is calculated for well 15 (approximately 150 km inland). At well 17 (220 km inland) the residence times increase up to the million year range. Uncertainty also exists in these estimates. C_0 as the initial Cl^- concentration was taken as an average value of all samples. Doing the same calculation with the average values for the single aquifers, 327 mg L^{-1} for aquifer C and 274 mg L^{-1} for aquifer D, would result in residence

times that can deviate up to more than ±70% from the numbers given in Table 4.

5.4. Summary discussion of the groundwater residence times

The ^{36}Cl groundwater residence times in the central Najd are in the same range as the ^{4}He ages shown in Table 3. The estimated ^{4}He and ^{36}Cl ages increase with flow distance, while a general trend of decreasing ^{14}C-DIC concentrations in the flow direction cannot be observed.

High ^{14}C-DIC concentrations in wells far from the recharge area indicate that mixing with a young component (dissolved in water or as gas phase) influences some of the wells. This has to be taken into account for the other age tracers as well. As the process as well as the magnitude of the mixing remains unknown, the effect on age estimates can only be discussed qualitatively. Admixture of a young, ^{4}He-poor component (or diffusive loss of ^{4}He to the vadose zone) would results in an underestimation of ages derived by ^{4}He concentrations. In same way, adding a ^{36}Cl-rich component would lead to an underestimation of ^{36}Cl-derived groundwater ages. Hence, the discrepancy between ^{14}C-DIC ages will be increased rather than minimized. Therefore, the estimated mean ages from ^{4}He (and ^{36}Cl) presented here (Tables 3 and 4) represent minimum ages.

Both, ^{4}He and ^{36}Cl, result in groundwater residence times of several hundred thousand years in the central Najd (80–150 km inland) and up to the million year range in the far distant area (>200 km). The resulting apparent groundwater flow velocities range from 0.1 to 3.5 m a^{-1}. Even when considering that the assumption of an ideal flow path (Table 1, distance of wells from the recharge area) does not reflect reality and spatial variations in the apparent groundwater velocities exist, the fact is that the UER aquifer contains very old groundwater.

These low groundwater velocities do not necessarily have to be in contradiction to the high transmissivities described above. It might be that more rapid groundwater velocities in the solution channels (aquifer C) appear. Especially under todays ‘pumped’ conditions, preferential flow along such structures can occur, leading to lower groundwater residence times in places or to mixtures of water of different age. However, this is not the main characteristic of the Najd groundwater flow system showing a significant piezometric gradient from the Mountains into the Najd. The low input due to limited recent recharge indicates a system of slow groundwater flow. Moreover, regional transmissivities might be much lower than the values obtained from (local) pumping tests so far. The difference between “early” and “late” estimates for the transmissivity has been discussed above. The “late” estimates refer to measured drawdowns for a time period of up to 3 days (at maximum). With that they still give very local statements. For a regional significance of the transmissivity pumping test up to several months are necessary.

The estimated time scale for the Najd groundwater indicates that the aquifers may have recharge from about ten glacial cycles. This means, among other things, that the aquifers were recharged under different recharge scenarios, most likely with varying rainfall intensity and, this cannot be excluded, changing moisture sources. It is undisputed that more humid conditions existed in the past, the large wadi channels pervading the ground from the Dhofar Mountains in direction north-east are a clear sign for that. It is understood that the monsoon reached farther to the north during humid periods in the past (Weyhenmeyer et al., 2000; Neff, 2001), while the varying monsoon intensity in southern Oman has been verified by stalagmite growth (Fleitmann et al., 2003a,b). On the other hand, the occurrence of different weather systems in the past (such as today's cyclones) and their impact on the deep groundwater system is unclear yet. The depleted signature of the stable isotopes at the far distant wells could be an indication for different weather systems and consequently different recharge sources. The same holds true for chloride with smaller concentrations and less variation in the distant wells.

While the sources of recharge might be unclear, the area where recharge to the deep aquifers could and can take place is clear. The recharge zone for the aquifers C and D stays the same at dry and wet conditions and is limited to the area close to the mountains. This is confirmed by the confined conditions of the aquifers, the fact that artesian outflow at the land surface occurs still today, and the upward gradient (higher water level in C and D then in the shallow aquifers). Even when surface runoff far inland occurred, infiltration to the deeper layers is unlikely.

The transients in the recharge rate, high during humid times and low during dry times, led to varying heads and varying flow conditions. Water levels in the Dhofar Mountains were most likely higher during humid periods and resulted in increased hydraulic-head gradients and a higher flow rate. During dry periods the head gradient decreased and less water was pushed through the aquifer. This means that the distance the water travelled in a fixed time period changed (and currently changes) with the transients in the recharge rate. The age pattern we see for the Najd groundwater comprises these periods of high and low flow. But since extent, duration and succession remain unknown they can only be discussed qualitatively.

Since the ^{4}He and ^{36}Cl age estimates are substantially higher than the previously valid ^{14}C residence times, we have been focusing on influences and processes which could alter the tracer signature. Underlying the limestones of the UER aquifer is a shale layer; embedded layers in the aquifers separating the water bearing horizons are also described as shale. Depending on the properties of the different rock material, leakage from the shale could influence the ^{4}He concentrations in the limestone aquifers. One way to identify the sources of ^{4}He$_{rad}$ is the comparison of measured ^{3}He and ^{4}He concentrations and the calculated production rates for both isotopes (Lehmann et al., 2003; Pearson et al., 1991). This requires, among other things, the lithium concentration of the rock material. Since these were not available for the Najd geological layers, literature values (Ahrens, 1965; Pearson et al., 1991) were used for calculating the ^{3}He/^{4}He production lines for limestone and

Table 4
^{36}Cl ages using an initial value of 17.1 × 10^{-15} at at^{-1}, minimum ages with R_{se} = 0, maximum ages with R_{se} = 9.5 × 10^{-15} at at^{-1} and C_0 = 302 mg L^{-1}.

Well	^{36}Cl/Cl (10^{-15} at at^{-1})	Cl (mg L^{-1})	R_{se} (10^{-15} at at^{-1})		R_{se} (10^{-15} at at^{-1})	
			0		9.5	
			^{36}Cl age (ka)	Age range (ka)	^{36}Cl age (ka)	Age range (ka)
12	14.1 ± 1.8	296	93	41–153	230	86–447
15	15.2 ± 1.6	273	94	50–144	168	58–315
17	9.7 ± 1.4	307	240	183–305	1664	693–1654[a]

[a] No upper limit could be calculated since analyzed value minus uncertainty is below R_{se}.

shale. By using these values the measured range for ^{3}He and ^{4}He was covered, but a clear distinction could not been made. Also, other available data fail to clarify the helium sources. A correlation of higher helium concentrations with higher Cl^{-} values as observed in other study areas (Lehmann et al., 1995) does not exist for the Najd samples.

It should be noted that the proportion of the various helium sources on the total concentration changes along the flow path. This applies to the *in-situ* production, which is of greater influence at the beginning of the flow path, as well as to the sources from outside the aquifer. The influence of the crustal flux increases with distance. In the central area (well 12) the residence times based on *in-situ* ^{4}He and ^{36}Cl are actually quite similar, which means that the crustal helium flux is of minor influence. The quite high *in-situ* ^{4}He residence times further downstream (well 17) on the other hand point to an additional helium source. *In-situ* ^{4}He as the only source overestimates the residence times in this area.

Leakage from confining or embedded layers can occur steadily along the flow path but can also act as point sources for helium, for example at locally higher U and Th amounts or due to a different rock matrix with varying lithium values. Another example for point sources could be the mentioned geological faults. An increased He flux from the depth, mixing of different water like pore water from high permeable and less permeable formations, or water from deeper aquifers, could result in higher ^{4}He concentrations and, thus, lead to an overestimation of the groundwater residence times. While it cannot be ruled out that the Najd samples are influenced by these factors, a clear indication for a dominant contribution is not given. In spite of all difficulties, the observed accumulation of ^{4}He shows the expected pattern and is supported by the interpretation of another independent tracer, ^{36}Cl.

In contrast to increasing ^{4}He concentrations with increasing distance or residence times, $^{36}Cl/Cl$ ratios are expected to decrease from a higher (initial) ratio to lower ratios downstream. Processes affecting ^{36}Cl deposition or ^{36}Cl and Cl^{-} production in the subsurface have been named above. The $^{36}Cl/Cl$ evolution of the Najd groundwater samples can be explained by these processes. However, a particularly crucial point is the choice of the initial $^{36}Cl/Cl$ ratio, followed by the assumption that this ratio is applicable for the samples along the flow path and with that for a time frame of several hundred thousands of years. It has been discussed above that the recharge conditions for the Najd, and not unlikely, also the recharge sources changed over time. Previous studies showed that the variability in ^{36}Cl concentrations and deposition rates can depend on the environmental conditions, for instance precipitation amounts (Knies et al., 1994; Phillips, 2000, 2013). Since the $^{36}Cl/Cl$ ratio is influenced by both, the ^{36}Cl and the stable Cl deposition, it has also to be considered that raising and lowering sea level over time influenced the Cl deposition, and with that the $^{36}Cl/Cl$ ratio of the groundwater recharge. Moysey et al. (2003) showed an inverse correlation of the $^{36}Cl/Cl$ ratio and stable Cl deposition for groundwater in the United States. However, the influences that might have controlled the $^{36}Cl/Cl$ recharge ratios for the Najd groundwater in the past cannot be estimated with the available data.

A further issue is the $^{36}Cl/Cl$ ratio of well 2 (17.1×10^{-15} at at^{-1}) used in the present study as the initial ratio R_0. Literature values show a wide range, often being above 100×10^{-15} at at^{-1} (for example 125×10^{-15} at at^{-1} for the Great Artesian Basin (Love et al., 2000). In areas near the sea, the $^{36}Cl/Cl$ ratio can be much lower because of the contribution dead chloride from the sea. Scheiber et al. (2015) for example selected 38×10^{-15} at at^{-1} for R_0, for a study in southern Spain. According to the ^{14}C age estimate for well 2 (4.4 ± 2.0 ka) and considering the half-life of ^{36}Cl, the ratio of well 2 (17.1×10^{-15} at at^{-1}) would represent today's initial $^{36}Cl/Cl$ ratio for the Dhofar area. On the one hand, values in the range of well 2 can be calculated as initial values for the Najd and today's climate conditions. On the other hand, the question arises if today's arid value is a representation for humid recharge conditions or if the well 2 water was recharged during conditions similar to today. In the present study, the $^{36}Cl/Cl$ ratio of well 2 was chosen as C_0 because of the position of well 2 at the beginning of the flow path, the relatively low ^{14}C age estimate and the low ^{4}He concentration. This leads to a reasonable explanation of the age pattern along the flow path, but it has to be reconsidered that variations in C_0 - which may have occurred in the past - had to be ignored for this interpretation.

It has been mentioned that paleoclimate implications, such as transients in the recharge rate, and their impact on the groundwater system (tracer ages) can only be discussed qualitatively. This holds also true for the localization of the Last Glacial Maximum (LGM). According to the ^{14}C age estimates the LGM should be located somewhere between well 2 and well 3, around the first 20 km along the flow path. Further evidence, for example a depleted stable isotope composition, cannot be detected. However, our interpretation is that the variations in the stable isotopes and the chloride especially at the first 100 km along the flow path, are indications for changing environmental conditions and that more than one glacial/interglacial period affected the recharging water.

One reason for the restricted interpretation here, of course, is that no sampling locations exist between km 20 (well 5) and km 67 (well 6). This limitation of not evenly distributed sampling locations applies to the whole study area. Further uncertainties could arise due the varying well completion. In addition, the pumping of the wells, especially in the farming areas starting at approximately 70 km inland, influences the natural (groundwater) system irreversibly. For a better understanding future work should focus on the recharge area and the area between well 5 and well 8. Besides the fact that little is known about the groundwater in these areas, it is also of advantage that these areas close to the mountains are less subject to abstraction. Artificial pollution or mixing should, therefore, have less influence.

It was known from previous investigations that the Najd groundwater is non-renewable on human timescales. The result of our study is that the groundwater residence times are even longer and reach up to >1 Ma including obviously groundwater recharged in different time periods. As it seems inevitable that groundwater abstraction will take place on a large scale in the Najd, it is nonetheless important to undertake measures from a water management perspective. For example, monitoring of abstraction rates at the discharge wells is absolutely essential. Besides the information what water volume is actually taken out of the aquifers, it will provide invaluable information for the parameter estimation of the aquifers.

6. Conclusions

Groundwater in southern Oman was investigated by a multi-isotope approach using stable water isotopes, ^{4}He, ^{14}C and ^{36}Cl and including hydrochemistry.

The use of multiple old age tracers in this study was critical to the final interpretation of the groundwater system, where different tracers were more applicable along different sections of the flow-path (Fig. 10). The ^{14}C ages appear to be most interpretable in the region most proximal to the recharge area where ages are 20 ka or less. It appears that the more distal samples have been compromised by well completions that are long open boreholes or are inadequately sealed.

^{4}He ages reveal much older values (>2 Ma at the distal end of the flow path), but uncertainty in the contributions of crustal

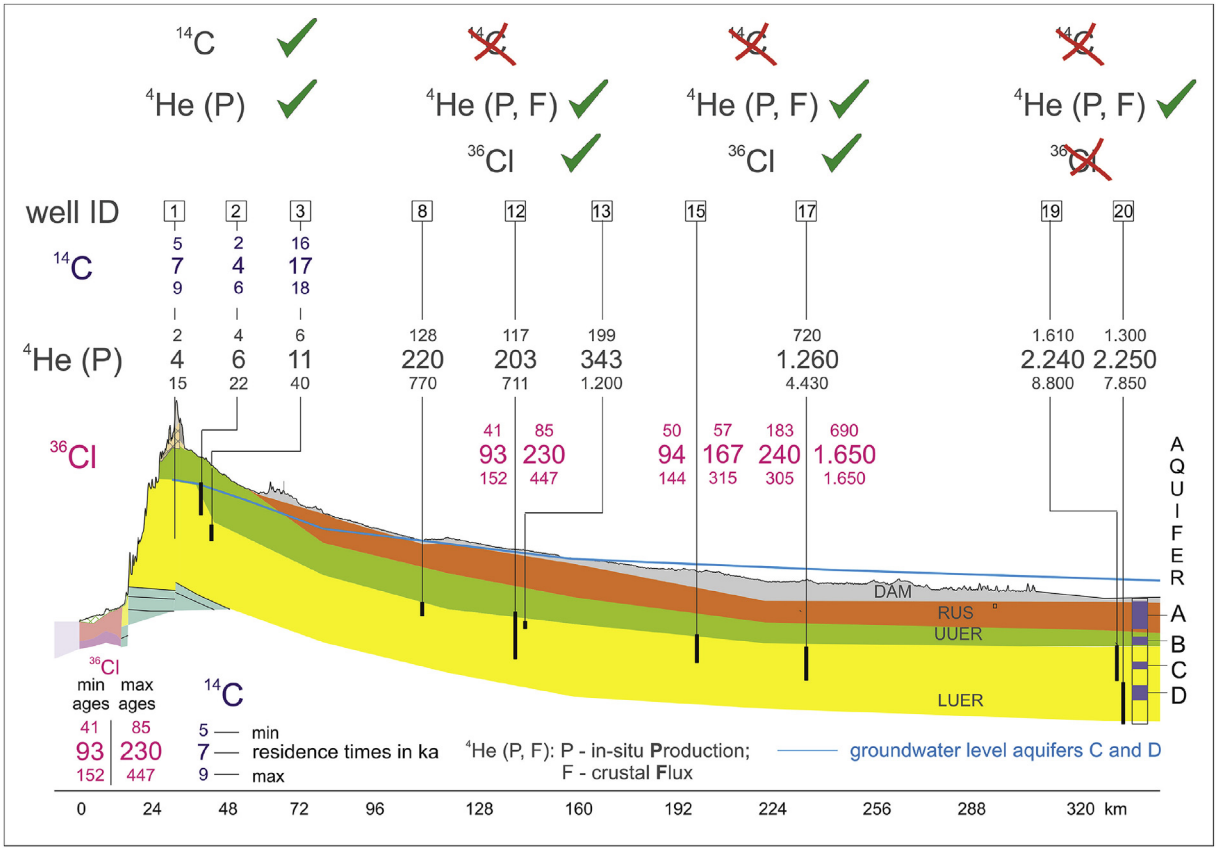

Fig. 10. Suitability and residence times of all tracers along the flow path. ^{14}C is only applicable in the first 20 km, while further downstream ^{4}He and ^{36}Cl allow the estimation of the residence times. The proportion of crustal helium (F) on the total ^{4}He increases along the flow path. Residence times based on in-situ ^{4}He only overestimate the ages in the far distant wells.

helium entering the base of the aquifer suggests that these oldest ages are a maximum value. ^{36}Cl analyses are consistent with the ^{4}He age estimates, and suggest that up to the central area the crustal helium flux into the aquifers of the UER is not a substantial fraction of the total helium present. The age range of up to >1 Ma is in contrast to earlier studies that only used ^{14}C data and concluded that the groundwater was recharged mostly during the LGM circa 20 ka ago. Deuterium and oxygen-18 data indicate that both tropical cyclones and seasonal monsoon rainfall in the Dhohar Mountains are sources of recharge. The study is an example of where multiple lines of chemical isotopic evidence can yield results different from those that rely dominantly on a single tracer set of data.

Acknowledgements

The authors would like to thank the laboratory team from the UFZ department Catchment Hydrology for the hydrochemical and stable isotope analyses. We are grateful for valuable discussions concerning the interpretation with N. Plummer and P. Fritz. We thank the DREAMS operator team and S. Akhmadaliev for help with AMS measurements at the HZDR Ion Beam Centre (IBC). We also wish to thank the Ministry of Water Resources for their steady support. Many thanks to the IPSWat Programm and the Helmholtz Interdisciplinary Graduate School for Environmental Research (HIGRADE). Any use of trade, firm, or product names is for descriptive purposes only and does not imply endorsement by the U.S. Government.

Appendix A. Supplementary data

Supplementary data related to this article can be found at http://dx.doi.org/10.1016/j.apgeochem.2016.08.012.

References

Abdul-Wahab, S.A., 2003. Analysis of thermal inversions in the khareef salalah region in the sultanate of Oman. J. Geophys. Res. Atmos. 108 (D9).
Aeschbach-Hertig, W., Gleeson, T., 2012. Regional strategies for the accelerating global problem of groundwater depletion. Nat. Geosci. 5 (12), 853–861.
Aeschbach-Hertig, W., Peeters, F., Beyerle, U., Kipfer, R., 1999. Interpretation of dissolved atmospheric noble gases in natural waters. Water Resour. Res. 35 (9), 2779–2792.
Aeschbach-Hertig, W., Peeters, F., Beyerle, U., Kipfer, R., 2000. Palaeotemperature reconstruction from noble gases in ground water taking into account equilibration with entrapped air. Nature 405 (6790), 1040–1044.
Aeschbach-Hertig, W., Stute, M., Clark, J.F., Reuter, R.F., Schlosser, P., 2002. A paleotemperature record derived from dissolved noble gases in groundwater of the Aquia Aquifer (Maryland, USA). Geochimica Cosmochim. Acta 66 (5), 797–817.
Ahrens, L.H., 1965. Some observations on the uranium and thorium distributions in accessory zircon from granitic rocks. Geochimica Cosmochim. Acta 29 (6), 711–716.
Akhmadaliev, S., Heller, R., Hanf, D., Rugel, G., Merchel, S., 2013. The new 6MV AMS-facility DREAMS at Dresden. Nucl. Instrum. Methods Phys. Res. Sect. B Beam Interact. Mater. Atoms 294, 5–10.
Al-Mashaikhi, K.S.A., 2011. Evaluation of Groundwater Recharge in Najd Aquifers Using Hydraulics, Hydrochemical and Isotope Evidences. PhD thesis. Helmholtz Centre for Environmental Research, UFZ.
Al-Mashaikhi, K., Oswald, S., Attinger, S., Büchel, G., Knöller, K., Strauch, G., 2012. Evaluation of groundwater dynamics and quality in the Najd aquifers located in the Sultanate of Oman. Environ. Earth Sci. 66 (4), 1195–1211.
Andrews, J.N., Lee, D.J., 1979. Inert gases in groundwater from the Bunter Sandstone of England as indicators of age and palaeoclimatic trends. J. Hydrol. 41 (3), 233–252.

Bakiewicz, W., Milne, D.M., Noori, M., 1982. Hydrogeology of the Umm Er Radhuma aquifer, Saudi Arabia, with reference to fossil gradients. Q. J. Eng. Geol. Hydrogeol. 15 (2), 105–126.

Benson, B.B., Krause Jr., D., 1980. Isotopic fractionation of helium during solution: a probe for the liquid state. J. Solut. Chem. 9 (12), 895–909.

Bentley, H., Phillips, F.M., Davis, S.N., Habermehl, M.A., Airey, P.L., Calf, G.E., Elmore, D., Gove, H.E., Torgersen, T., 1986. Chlorine-36 dating of very old groundwater: the Great Artesian Basin, Australia. Water Resour. Res. 22 (13), 1991–2001 [in page nr. 96, 97, 127].

Beyerle, U., Aeschbach-Hertig, W., Imboden, D.M., Baur, H., Graf, T., Kipfer, R., 2000. A mass spectrometric system for the analysis of noble gases and tritium from water samples. Environ. Sci. Technol. 34 (10), 2042–2050.

Bretzler, A., Osenbrück, K., Gloaguen, R., Ruprecht, J.S., Kebede, S., Stadler, S., 2011. Groundwater origin and flow dynamics in active rift systems–A multi-isotope approach in the Main Ethiopian Rift. J. Hydrol. 402 (3), 274–289.

Cartwright, I., Weaver, T.R., Cendón, D.I., Fifield, L.K., Tweed, S.O., Petrides, B., Swane, I., 2012. Constraining groundwater flow, residence times, inter-aquifer mixing, and aquifer properties using environmental isotopes in the southeast Murray Basin, Australia. Appl. Geochem. 27 (9), 1698–1709.

Castro, M.C., Stute, M., Schlosser, P., 2000. Comparison of ^{4}He ages and ^{14}C ages in simple aquifer systems: implications for groundwater flow and chronologies. Appl. Geochem. 15 (8), 1137–1167.

Clark, I.D., 1987. Groundwater Resources in the Sultanate of Oman: Origin, Circulation Times, Recharge Processes and Paleoclimatology. Isotopic and Geochemical Approaches. PhD Thesis. Paris 11.

Clark, I.D., Fontes, J.C., 1990. Paleoclimatic reconstruction in northern Oman based on carbonates from hyperalkaline groundwaters. Quat. Res. 33 (3), 320–336.

Clark, I.D., Fritz, P., Quinn, O.P., Rippon, P.W., Nash, H., AL Said, S.B.B.G., 1987. Modern and fossil groundwater in an arid environment: a look at the hydrogeology of southern Oman. In: Proc. Symp. On Isotope Techniques in Water Resources Development. IAEA (Int. At. Energy Agency), Vienna, pp. 167–187.

Clarke, W.B., Jenkins, W.J., Top, Z., 1976. Determination of tritium by mass spectrometric measurement of 3 He. Int. J. Appl. Radiat. Isot. 27 (9), 515–522.

Craig, H., Lupton, J.E., Welhan, J.A., Poreda, R., 1978. Helium isotope ratios in Yellowstone and Lassen Park volcanic gases. Geophys. Res. Lett. 5 (11), 897–900.

Davis, S.N., Cecil, D., Zreda, M., Sharma, P., 1998. Chlorine-36 and the initial value problem. Hydrogeol. J. 6 (1), 104–114.

Fleitmann, D., Matter, A., 2009. The speleothem record of climate variability in Southern Arabia. Comptes Rendus Geosci. 341 (8), 633–642.

Fleitmann, D., Burns, S.J., Neff, U., Mangini, A., Matter, A., 2003a. Changing moisture sources over the last 330,000 years in Northern Oman from fluid-inclusion evidence in speleothems. Quat. Res. 60 (2), 223–232.

Fleitmann, D., Burns, S.J., Mudelsee, M., Neff, U., Kramers, J., Mangini, A., Matter, A., 2003b. Holocene forcing of the Indian monsoon recorded in a stalagmite from southern Oman. Science 300 (5626), 1737–1739.

Foster, S., Loucks, D.P., 2006. Non-renewable Groundwater Resources. A Guidebook on Socially Sustainable Management for Water Policy Makers. IHP Series on Groundwater, p. 10.

Freeze, R.A., Cherry, J.A., 1979. Groundwater, 1979. Printice-Hall Inc, Englewood Cliffs, NJ, p. 604 [in page nr. : 40].

Friedrich, R., 2007. Grundwassercharakterisierung mit Umwelttracern: Erkundung des Grundwassers der Odenwald-Region sowie Implementierung eines neuen Edelgas-Massenspektrometersystems. PhD Thesis. Heidelberg University, Heidelberg.

GRC, 2005. Drilling and Aquifer Testing Project in the Western Al Wusta (Najd) Desert, Oman. Final Report, unpublished. Technical report. Ministry of Regional Municipality and Water Resources (MRMWR), p. 40.

GRC, 2008. Drilling and Aquifer Testing Programme in the Dhofar Governorate. Technical report, unpublished. Geo resources Consultancy [in page nr. : 11, 12, 17, 19, 21, 32, 34, 38, 40].

Guendouz, A., Michelot, J.L., 2006. Chlorine-36 dating of deep groundwater from northern Sahara. J. Hydrol. 328 (3), 572–580.

Herb, C., 2011. Paleoclimate Study Based on Noble Gases and Other Environmental Tracers in Groundwater in Dhofar (Southern Oman). Master thesis. Insititute of Environmental Physics, University of Heidelberg.

Herczeg, A.L., Leaney, F.W., 2011. Review: environmental tracers in arid-zone hydrology. Hydrogeol. J. 19 (1), 17–29.

Hildebrandt, A., Al Aufi, M., Amerjeed, M., Shammas, M., Eltahir, E.A., 2007. Eco-hydrology of a seasonal cloud forest in Dhofar: 1. Field experiment. Water Resour. Res. 43 (10).

Kalin, R.M., 2000. Radiocarbon dating of groundwater systems. In: Environmental Tracers in Subsurface Hydrology (Pp. 111–144). Springer, US.

Kipfer, R., Aeschbach-Hertig, W., Peeters, F., Stute, M., 2002. Noble gases in lakes and ground waters. In: Porcelli, D., Ballentine, C., Wieler, R. (Eds.), Noble gases in Geochemistry and Cosmochemistry. Mineralogical Society of America, Geochemical Society, Washington, DC, pp. 615–700.

Knies, D.L., Elmore, D., Sharma, P., Vogt, S., Li, R., Lipschutz, M.E., et al., 1994. ^{7}Be, ^{10}Be, and ^{36}Cl in precipitation. Nucl. Instrum. Methods Phys. Res. Sect. B Beam Interact. Mater. Atoms 92 (1–4), 340–344.

Konikow, L.F., Kendy, E., 2005. Groundwater depletion: A global problem. Hydrogeol. J. 13 (1), 317–320.

Kreuzer, A., 2007. Paläotemperaturstudie mit Edelgasen im Grundwasser der Nordchinesischen Tiefebene Paleotemperaturestudy with noble gases in the North China Plain aquifer. PhD Thesis. Heidelberg University, Heidelberg.

Kulongoski, J.T., Hilton, D.R., Cresswell, R.G., Hostetler, S., Jacobson, G., 2008. Helium-4 characteristics of groundwaters from Central Australia: Comparative chronology with chlorine-36 and carbon-14 dating techniques. J. Hydrol. 348 (1), 176–194.

Lehmann, B.E., Loosli, H.H., Purtschert, R., Andrews, J.N., 1995. A comparison of chloride and helium concentrations in deep groundwaters. In: Proceedings of the Symposium on Isotopes in Water Resources Management, IAEA-SM-336/44, Vienna (Pp. 3–17).

Lehmann, B.E., Love, A., Purtschert, R., Collon, P., Loosli, H.H., Kutschera, W., et al., 2003. A comparison of groundwater dating with ^{81}Kr, ^{36}Cl and ^{4}He in four wells of the Great Artesian Basin, Australia. Earth Planet. Sci. Lett. 211 (3), 237–250.

Lisiecki, L.E., Raymo, M.E., 2005. A Pliocene-Pleistocene stack of 57 globally distributed benthic δ^{18}O records. Paleoceanography 20 (1).

Love, A.J., Herczeg, A.L., Sampson, L., Cresswell, R.G., Fifield, L.K., 2000. Sources of chloride and implications for ^{36}Cl dating of old groundwater, southwestern Great Artesian Basin, Australia. Water Resour. Res. 36 (6), 1561–1574.

Macumber, P.G., Barghash, B.G.S., Kew, G.A., Tennakoon, T.B., 1995. Hydrogeologic Implications of a Cyclonic Rainfall Event in Central Oman. Groundwater Quality. Chapman and Hall, London, pp. 87–97.

Mahara, Y., Habermehl, M.A., Hasegawa, T., Nakata, K., Ransley, T.R., Hatano, T., et al., 2009. Groundwater dating by estimation of groundwater flow velocity and dissolved ^{4}He accumulation rate calibrated by ^{36}Cl in the Great Artesian Basin, Australia. Earth Planet. Sci. Lett. 287 (1), 43–56.

Mamyrin, B.A., Tolstikhin, I.N., 1984. Helium Isotopes in Nature. Elsevier.

Merchel, S., Braucher, R., Alfimov, V., Bichler, M., Bourlès, D.L., Reitner, J.M., 2013. The potential of historic rock avalanches and man-made structures as chlorine-36 production rate calibration sites. Quat. Geochronol. 18, 54–62.

Mott MacDonald International Ltd, 1991. Detailed Investigation for Development of up to 1000 ha of Irrigated Land: Nejd Region. Hydrogeology. Interim Report. Ministry of Agriculture and Fisheries, Sultanate of Oman.

Moysey, S., Davis, S.N., Zreda, M., Cecil, L.D., 2003. The distribution of meteoric ^{36}Cl/Cl in the United States: a comparison of models. Hydrogeol. J. 11 (6), 615–627.

Neff, U., 2001. Massenspektrometrische Th/U-Datierung von Höhlensintern aus dem Oman: Klimaarchive des asiatischen Monsuns. PhD thesis. Heidelberg University.

Nica, N., Cameron, J., Singh, B., 2012. Nuclear Data Sheets for A = 36. Nucl. Data Sheets 113, 1-155.

Ozima, M., Podosek, F.A., 2002. Noble gas Geochemistry. Cambridge University Press.

Pavetich, S., Akhmadaliev, S., Arnold, M., Aumaître, G., Bourlès, D., Buchriegler, J., et al., 2014. Interlaboratory study of the ion source memory effect in ^{36}Cl accelerator mass spectrometry. Nucl. Instrum. Methods Phys. Res. Sect. B Beam Interact. Mater. Atoms 329, 22–29.

Pearson, F.J., Balderer, W., Loosli, H.H., Lehmann, B.E., Matter, A., Peters, T., Gautschi, R.U. (Eds.), 1991. Applied Isotope Hydrogeology: A Case Study in Northern Switzerland. Elsevier [in page nr. : 88, 95, 96, 97, 112].

Phillips, F.M., 2000. Chlorine-36. In: Environmental Tracers in Subsurface Hydrology (Pp. 299–348). Springer, US.

Phillips, F. M. (2013). Chlorine-36 dating of old groundwater. In IAEA, 2013, Isotope Methods for Dating Old Groundwater, International Atomic Energy Agency, Vienna, April, 2013, Chap. 12. STI/PUB/1587, ISBN 978–92–0–137210–9, 357p.

Phillips, F.M., Bentley, H.W., Davis, S.N., Elmore, D., Swanick, G.B., 1986. Chlorine 36 dating of very old groundwater: 2. Milk River aquifer, Alberta, Canada. Water Resour. Res. 22 (13), 2003–2016.

Plummer, L. N., & Glynn, P. D. (2013). Radiocarbon dating in groundwater systems. In IAEA, 2013, Isotope Methods for Dating Old Groundwater, International Atomic Energy Agency, Vienna, April, 2013, Chap. 4. STI/PUB/1587, ISBN 978–92–0–137210–9, 357p.

Plummer, L.N., Prestemon, E.C., Parkhurst, D.L., 1994. An Interactive Code (NETPATH) for Modeling Net Geochemical Reactions along a Flow Path Version 2.0: US Geological Survey Water-resources Investigations Report 94-4169, Reston, Virginia.

Plummer, M.A., Phillips, F.M., Fabryka-Martin, J., Turin, H.J., Wigand, P.E., Sharma, P., 1997. Chlorine-36 in fossil rat urine: an archive of cosmogenic nuclide deposition during the past 40,000 years. Science 277 (5325), 538–541.

Plummer, L.N., Eggleston, J.R., Andreasen, D.C., Raffensperger, J.P., Hunt, A.G., Casile, G.C., 2012. Old groundwater in parts of the upper Patapsco aquifer, Atlantic Coastal Plain, Maryland, USA: evidence from radiocarbon, chlorine-36 and helium-4. Hydrogeol. J. 20 (7), 1269–1294.

Purdy, C.B., Helz, G.R., Mignerey, A.C., Kubik, P.W., Elmore, D., Sharma, P., Hemmick, T., 1996. Aquia Aquifer Dissolved Cl– and ^{36}Cl/Cl: implications for flow velocities. Water Resour. Res. 32 (5), 1163–1171.

Rosenberg, T.M., Preusser, F., Fleitmann, D., Schwalb, A., Penkman, K., Schmid, T.W., et al., 2011. Humid periods in southern Arabia: windows of opportunity for modern human dispersal. Geology 39 (12), 1115–1118.

Rugel, G., Pavetich, S., Akhmadaliev, S., Baez, S.M.E., Scharf, A., Ziegenrücker, R., Merchel, S., 2016. The first four years of the AMS-facility DREAMS: Status and developments for more accurate radionuclide data. Nucl. Instrum. Methods Phys. Res. Sect. B Beam Interact. Mater. Atoms 370, 94–100.

Sanford, W.E., Plummer, L.N., McAda, D.P., Bexfield, L.M., Anderholm, S.K., 2004. Hydrochemical tracers in the middle Rio Grande Basin, USA: 2. Calibration of a groundwater-flow model. Hydrogeol. J. 12 (4), 389–407.

Scanlon, B.R., Faunt, C.C., Longuevergne, L., Reedy, R.C., Alley, W.M., McGuire, V.L., McMahon, P.B., 2012. Groundwater depletion and sustainability of irrigation in the US High Plains and Central Valley. Proc. Natl. Acad. Sci. U. S. A. 109 (24), 9320–9325.

Scheiber, L., Ayora, C., Vázquez-Suñé, E., Cendón, D.I., Soler, A., Custodio, E., Baquero, J.C., 2015. Recent and old groundwater in the Niebla-Posadas regional aquifer (southern Spain): Implications for its management. J. Hydrol. 523, 624–635.

Schemenauer, R.S., Cereceda, P., 1992. Monsoon cloudwater chemistry on the Arabian Peninsula. Atmos. Environ. Part A. General Top. 26 (9), 1583–1587.

Schimmelpfennig, I., Benedetti, L., Finkel, R., Pik, R., Blard, P.H., Bourles, D., et al., 2009. Sources of in-situ ^{36}Cl in basaltic rocks. Implications for calibration of production rates. Quat. Geochronol. 4 (6), 441–461.

Siebert, S., Burke, J., Faures, J.M., Frenken, K., Hoogeveen, J., Döll, P., Portmann, F.T., 2010. Groundwater use for irrigation–a global inventory. Hydrol. Earth Syst. Sci. 14 (10), 1863–1880.

Solomon, D.K., Cook, P.G., 2000. 3h and 3he. In: Environmental Tracers in Subsurface Hydrology (Pp. 397–424). Springer, US.

Solomon, D.K., Hunt, A., Poreda, R.J., 1996. Source of radiogenic helium 4 in shallow aquifers: Implications for dating young groundwater. Water Resour. Res. 32 (6), 1805–1813.

Stadler, S., Osenbrück, K., Suckow, A.O., Himmelsbach, T., Hötzl, H., 2010. Groundwater flow regime, recharge and regional-scale solute transport in the semi-arid Kalahari of Botswana derived from isotope hydrology and hydrochemistry. J. Hydrol. 388 (3), 291–303.

Strauch, G., Al-Mashaikhi, K.S., Bawain, A., Knöller, K., Friesen, J., Müller, T., 2014. Stable H and O isotope variations reveal sources of recharge in Dhofar, Sultanate of Oman. Isot. Environ. health Stud. 50 (4), 475–490.

Sturchio, N., & Purtschert, R. (2013). Krypton-81 case study: the Nubian aquifer, Egypt. In IAEA, 2013, Isotope Methods for Dating Old Groundwater, International Atomic Energy Agency, Vienna, April, 2013, Chap. 14. STI/PUB/1587, ISBN 978–92–0–137210–9, 357p.

Stute, M., Sonntag, C., Déak, J., Schlosser, P., 1992. Helium in deep circulating groundwater in the Great Hungarian Plain: Flow dynamics and crustal and mantle helium fluxes. Geochimica Cosmochim. Acta 56 (5), 2051–2067.

Torgersen, T., 2010. Continental degassing flux of 4He and its variability. Geochem. Geophys. Geosystems 11 (6) [in page nr. : 116, 118].

Torgersen, T. (2013). Methods for dating very old groundwater: eastern and central Great Artesian Basin case study. In IAEA, 2013, Isotope Methods for Dating Old Groundwater, International Atomic Energy Agency, Vienna, April, 2013, Chap. 13. STI/PUB/1587, ISBN 978–92–0–137210–9, 357p.

Torgersen, T., Clarke, W.B., 1985. Helium accumulation in groundwater, I: An evaluation of sources and the continental flux of crustal 4 He in the Great Artesian Basin, Australia. Geochimica Cosmochim. Acta 49 (5), 1211–1218.

Unkel, I., 2006. AMS-14C-Analysen zur Rekonstruktion der Landschafts-und Kulturgeschichte in der Region Palpa (S-Peru). Heidelberg University, Heidelberg. PhD Thesis.

von Rohden, C., Kreuzer, A., Chen, Z., Kipfer, R., Aeschbach-Hertig, W., 2010. Characterizing the recharge regime of the strongly exploited aquifers of the North China Plain by environmental tracers. Water Resour. Res. 46 (5).

Wada, Y., van Beek, L.P., van Kempen, C.M., Reckman, J.W., Vasak, S., Bierkens, M.F., 2010. Global depletion of groundwater resources. Geophys. Res. Lett. 37 (20).

Weyhenmeyer, C.E., Burns, S.J., Waber, H.N., Aeschbach-Hertig, W., Kipfer, R., Loosli, H.H., Matter, A., 2000. Cool glacial temperatures and changes in moisture source recorded in Oman groundwaters. Science 287 (5454), 842–845.

Wieser, M., 2010. Imprints of Climatic and Environmental Change in a Regional Aquifer System in an Arid Part of India Using Noble Gases and Other Environmental Tracers. PhD Thesis. Heidelberg University, Heidelberg.

WWAP (United Nations World Water Assessment Programme), 2015. The United Nations World Water Development Report 2015: Water for a Sustainable World. UNESCO, Paris.

Zuber, A., Weise, S.M., Osenbrueck, K., Mateńko, T., 1997. Origin and age of saline waters in Busko Spa (Southern Poland) determined by isotope, noble gas and hydrochemical methods: evidence of interglacial and pre-Quaternary warm climate recharges. Appl. Geochem. 12 (5), 643–660.